THE ASTRONOMICAL JOURNAL VOLUME 112, NUMBER 6 DECEMBER 1996

CARBON STARS IN THE LARGE MAGELLANIC CLOUD: LUMINOSITIES, COLORS, AND IMPLICATIONS FOR THE HISTORY OF STAR FORMATION

EDGARDO COSTA[1]
Departamento de Astronomia, Universidad de Chile, Casilla 36-D, Santiago, Chile
Electronic mail: costa@das.uchile.cl

JAY A. FROGEL[2,3]
Cerro Tololo InterAmerican Observatory, Casilla 603, La Serena, Chile
Electronic mail: frogel@galileo.mps.ohio-state.edu

Received 1996 July 3; revised 1996 August 21

ABSTRACT

We present *RI* and *JHK* photometry for 888 and 204 carbon (C) stars, respectively, of the 1035 C stars found by Blanco and his collaborators in 52 fields of the Large Magellanic Cloud (LMC). The results of our analysis of the data fall into two categories: (1) Derivation of the physical properties of the stars and a comparison with models. (2) The variation in C star properties with position in the LMC and implications for the history of star formation. For the 197 stars with data in all 5 photometric bands, we derive an equation that gives $m_{\rm bol}$ (± 0.34 mag) from the R_0 and I_0 data alone. With $m_{\rm bol}$ for 895 LMC C stars we derive a luminosity function that is closely similar to those for previous (but an order of magnitude smaller) samples of both field and cluster LMC C stars. We find only two C stars brighter than $m_{\rm bol}=12.5$ and fewer than 10 fainter than 15.5. A comparison of our derived bolometric magnitudes and effective temperatures for the LMC C stars with the models of Lattanzio [ApJ, 311, 708 (1986); ApJS, 76, 215 (1991)] leads us to conclude that $\sim 1\ \mathcal{M}_\odot$ is the minimum mass required to produce a Population II C star. In addition, the observed lower limit we find to the C star luminosities corresponds to the luminosity at which a $1\ \mathcal{M}_\odot$ Pop II star is predicted to have its first major thermal pulse. From a comparison of field and cluster C star color–magnitude diagrams, we conclude that the range in age and metallicity of the LMC field C stars is at least as great as those from LMC clusters. The metallicity range of the field C stars, though, appears to extend to a significantly higher value based on our finding that red C stars with $(J-K)_0>1.9$ are three to four times more common in the field sample than in cluster stars and a similar difference previously noted between field and cluster M giants [Frogel & Blanco, ApJ, 365, 168 (1990)]. For each field observed we derive a luminosity $m_{\rm bol}(t)$ that should be related to the transition luminosity between M and C stars. We find that the $m_{\rm bol}(t)$ values are comparable to those found by FMB for SWB type V–VI clusters and are at least a magnitude fainter than those typical of SWB II–IV clusters. Furthermore, we find that these values of $m_{\rm bol}(t)$ get brighter with increasing distance of the field from the LMC's bar. Such a result would be expected if the upper limit to C star ages decreased as one approached the periphery of the LMC by an amount corresponding to an increase of $\sim 30\%$ in the minimum main-sequence-turnoff mass. We do not find any other statistically significant variations with position in the properties of the C stars. © *1996 American Astronomical Society.*

1. INTRODUCTION

For the past 15 years the Magellanic Clouds have provided an exceptionally fertile ground for the interplay of observations of asymptotic giant branch (AGB) stars, particularly carbon stars, and stellar evolution theory. This productive interaction has been possible because: (1) The extinction to both Clouds is low and relatively uniform. (2) The physical extent of both clouds along the lines of sight to them is only a few percent of their distance. (3) Both Clouds have significant numbers of populous star clusters whose ages and chemical compositions can be estimated to a useful degree of accuracy (and are closely related to one another, e.g., Cohen 1982; Bica *et al.* 1986) and which contain large numbers of AGB stars. (4) It has been possible to carry out large scale surveys for AGB stars in the Clouds, several of which, in particular those for C stars by Blanco *et al.* (1980, hereafter BMB), Blanco & McCarthy (1983, hereafter BM), and Rebeirot *et al.* (1993) are essentially complete and not magnitude limited. These four characteristics have allowed the straightforward testing of many key predictions of stellar evolution theory such as the definition of the luminosity

[1]Visiting Astronomer, Cerro Tololo InterAmerican Observatory, which is operated by AURA, Inc., under contract with the NSF.
[2]On the staff of CTIO when these observations were made. Permanent address: Department of Astronomy, The Ohio State University, 174 West 18th Avenue, Columbus, OH 43210.
[3]Also, Department of Physics, University of Durham, England.

 0004-6256/96/112(6)/2607/27/$10.00

function of AGB stars, its dependence on age and chemical composition, and the relative numbers of M, S, and C stars.

We have obtained *RI* photometry for an unbiased sample of ~900 of the more than 1000 C stars found by BM and BMB in 52 fields of the LMC and *JHK* photometry for ~200 of the stars with *RI* data. Our reasons for carrying out what may be the last such extensive program of single-star photoelectric photometry fall into two broad categories: first, to rederive the photometric properties of LMC C stars with a sample that is nearly an order of magnitude larger than any previous one and to compare these properties with predictions of stellar evolution theory; second, to see what can be learned about the history of star formation in the LMC by testing for variations in the properties of the C stars with position.

Section 2 describes our *RI* and *JHK* observations of the C stars drawn from the Blanco *et al.* surveys and discusses the derivation of bolometric magnitudes from these data. From these bolometric magnitudes we constructed what can be considered to be the definitive luminosity function for *N*-type noncluster C stars in the LMC; this is presented in Sec. 3. Also in Sec. 3 we describe and discuss color–magnitude and color–color diagrams for the C stars and make comparisons with other C star samples. Temperature estimates based on the colors are derived in Sec. 4; they and the bolometric magnitudes are compared with model predictions. A bolometric transition luminosity that should be closely related to that which marks the faint end of the C star and the bright end of the M star distribution is derived for each field in Sec. 5. We investigate whether this transition luminosity or any of the other parameters that characterize the C and late M stars is correlated with position within the LMC. A summary of our major results and some further discussion is contained in Sec. 6.

2. OBSERVATIONS AND BOLOMETRIC MAGNITUDES

2.1 Selection of the Carbon Star Sample

Blanco and his collaborators (BM & BMB) carried out low dispersion red grism surveys for C and M giants in 52 fields in the LMC each 0.12 deg^2 in size, distributed over an area of 8×8°. Of particular importance is that for C stars, and the later M giants, these surveys are not limited by apparent magnitude since the faintest C stars found are a magnitude or more brighter than the faint limit of the survey (the existence of a distinct population of C stars whose brightest members are below the survey limit and, hence, considerably fainter than the faintest C stars cannot be ruled out). Extensive blue spectroscopic surveys for C and CH stars (e.g., Westerlund *et al.* 1986; Hartwick & Cowley 1988; see also Feast & Whitlock 1992 and Suntzeff *et al.* 1993) have identified additional C stars that were missed by the Blanco *et al.* surveys because of their relatively bluer colors. While they are of comparable luminosity to the redder stars found by Blanco *et al.*, these blue stars appear to be rare and add at most a few percent to the total C star population. It also appears that the number of C stars that would have been missed by Blanco *et al.* due to dust obscuration (e.g., Frogel & Richer 1983; Reid *et al.* 1990; Groenewegen & de Jong 1993) is small. This is not to say that understanding the origin of these two groups of stars is not of some importance for interpreting the C star phenomenon in general (cf. Groenewegen & de Jong 1993). Finally, there is no evidence that any significant numbers of C or M stars are so bright that they would have been saturated on the survey plates.

Of the 1035 carbon stars identified by Blanco *et al.* in the LMC, 895 were observed by us. Table 1 lists the fields in which the observed stars are located together with the extinction values for each field derived as discussed in Sec. II d. Coordinates for the LMC field centers and a schematic view

TABLE 1. Reddening corrections.

Field	E(*BV*)	A_I	E(*RI*)	A_K	E(*JK*)	E(*HK*)
LMC BW	0.17	0.33	0.09	0.05	0.09	0.04
LMC O	0.12	0.23	0.07	0.03	0.07	0.03
LMC R	0.10	0.19	0.06	0.03	0.06	0.02
LMC 1	0.10	0.19	0.06			
LMC 2	0.10	0.19	0.06			
LMC 3	0.10	0.19	0.06			
LMC 5	0.12	0.23	0.07			
LMC 6	0.12	0.23	0.07			
LMC 7	0.07	0.13	0.04			
LMC 8	0.10	0.19	0.06			
LMC 9	0.12	0.23	0.07	0.03	0.07	0.03
LMC 10	0.10	0.19	0.06			
LMC 11	0.12	0.23	0.07			
LMC 12	0.12	0.23	0.07	0.03	0.07	0.03
LMC 13	0.10	0.19	0.06			
LMC 14	0.10	0.19	0.06			
LMC 16	0.17	0.33	0.09			
LMC 17	0.10	0.19	0.06			
LMC 18	0.10	0.19	0.06			
LMC 19	0.10	0.19	0.06			
LMC 20	0.10	0.19	0.06	0.03	0.06	0.02
LMC 21	0.12	0.23	0.07			
LMC 23	0.10	0.19	0.06			
LMC 24	0.10	0.19	0.06			
LMC 25	0.07	0.13	0.04			
LMC 27	0.10	0.19	0.06			
LMC 28	0.12	0.23	0.07			
LMC 29	0.10	0.19	0.06			
LMC 30	0.12	0.23	0.07			
LMC 31	0.10	0.19	0.07			
LMC 32	0.12	0.23	0.07	0.03	0.07	0.03
LMC 33	0.16	0.31	0.09	0.05	0.09	0.03
LMC 34	0.12	0.23	0.07			
LMC 35	0.10	0.19	0.06			
LMC 36	0.12	0.23	0.07			
LMC 37	0.12	0.23	0.07	0.03	0.07	0.03
LMC 38	0.18	0.35	0.10	0.05	0.10	0.04
LMC 39	0.10	0.19	0.06			
LMC 40	0.10	0.19	0.06			
LMC 41	0.10	0.19	0.06			
LMC 42	0.12	0.19	0.06			
LMC 43	0.12	0.23	0.07			
LMC 44	0.10	0.19	0.06			
LMC 45	0.10	0.19	0.06			
LMC 46	0.10	0.19	0.06			
LMC 47	0.07	0.13	0.04			
LMC 48	0.10	0.19	0.06			
LMC 49	0.07	0.13	0.04			
LMC 50	0.10	0.19	0.06			
LMC 51	0.10	0.19	0.06			
LMC 52	0.10	0.19	0.06			
WORC	0.10	0.19	0.06			

of their distribution can be found in BM. Identification charts and coordinates for the individual stars can be found in Blanco & McCarthy (1990) and in BMB. In addition to the Blanco *et al.* stars, 35 additional stars identified as C stars by Westerlund *et al.* (1978, hereafter WORC) in the outskirts of the LMC were observed. Finding charts and coordinates for these objects can be found in WORC. Mean extinction values for the LMC as a whole were applied to the WORC sample.

2.2 *RI* Kron–Cousins Photometry

RI photometry in the Kron–Cousins (kc) system was obtained for 888 of the stars in the surveys of BMB and BM, and for all 35 stars in the WORC sample. Some of the *RI* data (for fields LMC 12 and LMC 17) are from Costa (1990). These data, corrected for reddening as discussed below, are given in Tables 2(a) and 2(b). The last column of Table 2(a) indicates whether *JHK* data for the star are given in Table 3.

All of the *RI* observations were made with a dry-ice cooled GaAr Hamamatsu R943-02 photomultiplier. The *R* bandpass was defined with Schott 2 mm OG570+2 mm KG3 combination. The short-wavelength limit of the *I* bandpass was defined with a Schott 1 mm RG780+3 mm RG715 combination; its long-wavelength limit was set by the rapid loss of sensitivity of the Hamamatsu tube beyond $\lambda \sim 9000$ Å. These filter combinations closely (Graham 1982) reproduce the standard *RI*(kc) system defined by Cousins (1974, 1976a, 1978, 1980a, 1980b). About 90% of the *RI* observations were made during 1990 December and 1991 January at the *f*/13.5 focus of the CTIO 1.5 m telescope. The rest were made with the CTIO 1 m telescope in 1991 November–December and 1992 January. A 10″ aperture was used on the 1.5 m, while a 9.4″ aperture was employed on the 1 m. These sizes were chosen as a compromise between photometric accuracy and minimizing crowding.

About twelve *UBVRI* standard stars in the Harvard E regions (Graham 1982) were observed multiple times each night to determine the transformation of instrumental magnitudes to the standard *RI*(kc) system and the extinction corrections. The majority of the program stars were observed only once. With the exception of the faintest program stars, typical integration times in both colors were 20 s (1.5 m) and 60 s (1 m) which gave estimated precisions of 2%–3%. Reductions followed standard procedures (Hardie 1962). Further details may be found in Costa (1990).

2.3 *JHK* Photometry

Table 3 lists *JHK* data for 204 carbon stars in 10 fields from BMB and BM corrected for reddening as discussed below. *RI* observations for 197 of them are from Table 2(a). *JHK* data for stars in 7 of the fields were obtained in 1985 November with CTIO's D3 InSb system on the Blanco 4 m telescope. Data for C stars in the Bar West, Optical center, and Radio center fields (LMC BW, LMC O, and LMC R in Table 1), are from Cohen *et al.* (1981, hereafter CFPE) who employed an instrumental setup identical to that used here. All data are on the CIT/CTIO system (Elias *et al.* 1982). For those fields where it was not possible to observe every C star

TABLE 2. Reddening corrected *RI* photometry for Blanco *et al.* LMC carbon stars.

Star	$(R\ I)_0$	I_0	m_{bol}	*JHK*
LMC 01-1	0.96	14.57	14.53	
LMC 01-2	1.27	13.65	13.20	
LMC 01-3	1.26	14.37	13.93	
LMC 02-1	1.36	14.16	13.59	
LMC 02-2	1.13	14.62	14.36	
LMC 03-1	1.24	13.96	13.55	
LMC 03-2	1.07	13.75	13.57	
LMC 03-4	1.30	13.61	13.12	
LMC 03-5	1.18	13.84	13.51	
LMC 03-6	1.64	15.91	14.97	
LMC 03-7	1.36	14.08	13.51	
LMC 03-8	0.51	14.73	15.29	
LMC 05-1	0.85	14.02	14.13	
LMC 05-2	0.77	14.44	14.66	
LMC 05-3	1.17	13.91	13.59	
LMC 05-4	1.34	14.14	13.60	
LMC 05-5	1.11	14.33	14.09	
LMC 05-6	1.01	14.39	14.29	
LMC 05-7	1.09	13.68	13.47	
LMC 05-8	1.16	14.01	13.71	
LMC 05-9	0.90	14.42	14.46	
LMC 05-10	1.08	13.87	13.67	
LMC 05-11	1.28	13.19	12.73	
LMC 05-12	1.06	14.54	14.37	
LMC 06-1	0.95	14.12	14.10	
LMC 06-2	1.10	14.07	13.85	
LMC 06-3	1.05	13.97	13.81	
LMC 06-4	1.18	14.96	14.63	
LMC 06-5	0.90	13.97	14.01	
LMC 06-6	0.86	13.72	13.82	
LMC 06-7	1.20	13.78	13.42	
LMC 06-8	1.18	13.81	13.48	
LMC 06-9	0.72	14.47	14.75	
LMC 06-10	1.04	14.15	14.01	
LMC 06-11	1.02	14.37	14.25	
LMC 06-12	0.92	14.08	14.10	
LMC 06-14	1.14	13.88	13.60	
LMC 06-15	0.70	14.67	14.98	
LMC 06-16	1.23	13.92	13.52	
LMC 06-17	1.36	14.16	13.59	
LMC 06-18	1.17	13.86	13.54	
LMC 06-19	0.88	14.64	14.71	
LMC 06-20	0.94	13.52	13.51	
LMC 07-1	1.26	13.87	13.43	
LMC 07-2	0.91	14.88	14.91	
LMC 07-3	0.89	15.05	15.11	
LMC 07-4	1.24	13.89	13.48	
LMC 07-5	0.78	15.15	15.35	
LMC 07-6	1.05	13.95	13.79	
LMC 07-7	1.05	13.94	13.78	
LMC 07-8	1.09	14.14	13.93	
LMC 07-9	1.34	14.20	13.66	
LMC 07-10	1.20	13.82	13.46	
LMC 07-11	1.18	14.36	14.03	
LMC 08-1	0.89	14.07	14.13	
LMC 08-2	0.86	14.11	14.21	
LMC 08-3	0.93	12.88	12.88	
LMC 08-4	1.08	14.30	14.10	
LMC 08-5	0.94	14.14	14.13	
LMC 08-6	1.34	14.95	14.41	
LMC 09-2	1.28	13.69	14.15	yes
LMC 09-3	1.02	13.96	14.18	yes
LMC 09-4	0.89	13.92	14.08	yes
LMC 09-5	0.82	14.26	14.48	yes
LMC 09-6	0.95	14.23	14.04	yes
LMC 09-7	0.95	14.49	14.65	yes

TABLE 2. (continued)

Star	$(R\ I)_0$	I_0	m_{bol}	JHK	Star	$(R\ I)_0$	I_0	m_{bol}	JHK
LMC 09-8	1.39	13.68	13.17	yes	LMC 11-13	1.32	14.34	13.82	
LMC 09-9	1.03	13.59	13.60	yes	LMC 11-14	1.38	13.87	13.27	
LMC 09-10	1.08	13.84	13.64	yes	LMC 11-15	1.03	13.24	13.11	
LMC 09-11	1.05	13.77	13.59	yes	LMC 11-17	0.91	13.13	13.16	
LMC 09-12	1.05	13.80	13.68	yes	LMC 11-18	1.15	14.01	13.72	
LMC 09-13	1.05	13.54	13.69	yes	LMC 11-19	0.84	13.52	13.64	
LMC 09-14	0.86	13.76	13.67	yes	LMC 12-1	0.94	13.91	14.00	yes
LMC 09-15	0.48	13.56	13.67	yes	LMC 12-2	1.19	14.76	13.76	yes
LMC 09-16	1.00	13.89	13.86	yes	LMC 12-3	0.89	13.72	13.70	yes
LMC 09-17	1.07	13.84	13.76	yes	LMC 12-4	0.80	14.33	14.90	yes
LMC 09-18	0.92	13.20	13.30	yes	LMC 12-5	1.09	13.09	13.03	yes
LMC 09-19	1.32	14.28	12.93	yes	LMC 12-6	1.09	14.40	14.14	yes
LMC 09-20	1.25	14.24	13.78	yes	LMC 12-7	1.00	13.45	13.83	yes
LMC 09-21	0.89	14.65	14.53	yes	LMC 12-8	1.50	15.64	13.95	yes
LMC 09-22	0.59	13.44	14.71	yes	LMC 12-9	1.09	13.76	13.52	yes
LMC 09-23	1.07	14.15	14.16	yes	LMC 12-10	1.25	13.97	13.66	yes
LMC 09-25	1.45	14.19	13.87	yes	LMC 12-11	0.92	14.11	14.02	yes
LMC 09-26	0.90	13.95	14.87	yes	LMC 12-12	1.20	13.66	13.35	yes
LMC 09-27	1.20	14.46	14.38	yes	LMC 12-13	1.09	14.13	13.56	yes
LMC 09-28	1.27	13.65	13.75	yes	LMC 12-14	1.06	13.10	12.84	yes
LMC 09-29	0.99	13.35	13.50	yes	LMC 12-15	1.21	13.99	13.75	yes
LMC 09-30	1.19	13.68	14.05	yes	LMC 12-16	1.15	14.49	14.28	yes
LMC 09-31	0.91	13.70	14.17	yes	LMC 12-17	1.32	14.28	13.08	yes
LMC 09-32	1.15	14.01	14.11	yes	LMC 12-18	0.94	13.18	13.02	yes
LMC 10-1	0.99	13.30	13.22		LMC 12-19	0.61	12.64	12.68	yes
LMC 10-2	1.07	14.18	14.00		LMC 13-1	1.26	13.96	13.52	
LMC 10-3	1.39	14.12	13.51		LMC 13-2	1.12	14.54	14.29	
LMC 10-4	0.75	15.17	15.41		LMC 13-3	0.54	15.01	15.53	
LMC 10-5	0.95	13.89	13.87		LMC 13-4	0.97	14.02	13.97	
LMC 10-6	1.00	13.54	13.45		LMC 13-5	1.36	14.41	13.84	
LMC 10-7	1.45	14.46	13.77		LMC 13-6	0.93	13.35	13.35	
LMC 10-8	1.16	13.42	13.12		LMC 13-7	1.06	13.57	13.40	
LMC 10-9	1.71	14.48	13.45		LMC 13-8	0.51	16.10	16.66	
LMC 10-10	0.97	13.25	13.20		LMC 13-9	1.25	13.61	13.19	
LMC 10-11	0.90	13.72	13.76		LMC 13-10	1.23	13.99	13.59	
LMC 10-12	0.91	14.21	14.24		LMC 13-11	0.72	14.69	14.97	
LMC 10-13	0.93	13.78	13.78		LMC 13-12	1.00	13.64	13.55	
LMC 10-14	1.23	13.72	13.32		LMC 13-13	0.94	13.96	13.95	
LMC 10-15	0.87	14.43	14.51		LMC 13-14	1.15	14.67	14.38	
LMC 10-16	1.06	13.63	13.46		LMC 13-15	1.11	13.76	13.52	
LMC 10-17	1.03	14.39	14.26		LMC 13-16	0.64	14.66	15.05	
LMC 10-18	1.01	13.91	13.81		LMC 13-17	1.31	13.84	13.34	
LMC 10-19	0.88	14.76	14.83		LMC 13-18	1.02	13.34	13.22	
LMC 10-20	0.91	13.68	13.71		LMC 14-1	1.06	14.27	14.10	
LMC 10-21	1.19	14.88	14.54		LMC 14-2	0.89	13.59	13.65	
LMC 10-22	0.84	14.19	14.31		LMC 14-3	1.02	13.51	13.39	
LMC 10-23	0.99	14.20	14.12		LMC 14-4	0.93	13.84	13.84	
LMC 10-24	0.89	13.34	13.40		LMC 14-5	0.75	14.17	14.41	
LMC 10-25	1.21	14.24	13.87		LMC BW-1	1.47	16.14	13.92	yes
LMC 10-26	0.83	13.57	13.71		LMC BW-3	1.01	13.47	13.24	yes
LMC 10-27	0.89	13.94	14.00		LMC BW-5	1.16	13.74	13.44	
LMC 10-28	1.12	14.93	14.68		LMC BW-6	0.94	14.10	14.09	
LMC 10-29	1.11	14.34	14.10		LMC BW-8	1.04	13.39	13.25	
LMC 10-30	1.20	13.86	13.50		LMC BW-9	0.99	14.59	14.61	yes
LMC 10-31	1.29	13.74	13.26		LMC BW-11	1.20	13.61	13.14	yes
LMC 10-32	1.10	13.90	13.68		LMC BW-13	1.20	13.93	13.57	
LMC 11-1	0.73	13.67	13.94		LMC BW-15	0.99	13.71	13.63	
LMC 11-2	1.01	14.36	14.26		LMC BW-18	0.96	13.31	13.27	
LMC 11-3	1.36	13.85	13.28		LMC BW-19	0.94	13.90	13.86	yes
LMC 11-4	0.86	15.60	15.70		LMC BW-21	1.12	13.78	13.71	yes
LMC 11-5	1.15	14.15	13.86		LMC BW-23	1.48	14.08	13.35	
LMC 11-6	1.13	13.64	13.38		LMC BW-24	1.32	14.37	13.44	yes
LMC 11-7	1.06	13.59	13.42		LMC BW-25	1.25	13.45	13.11	yes
LMC 11-8	1.31	13.53	13.03		LMC BW-28	0.96	13.89	13.85	
LMC 11-10	1.24	13.96	13.55		LMC BW-29	0.88	13.85	13.92	
LMC 11-11	0.58	14.26	14.73		LMC BW-31	1.00	14.17	14.08	
LMC 11-12	1.03	14.07	13.94		LMC BW-32	1.00	13.67	13.58	

TABLE 2. (continued)

Star	$(R\ I)_0$	I_0	m_{bol}	JHK	Star	$(R\ I)_0$	I_0	m_{bol}	JHK
LMC BW-33	0.99	14.23	14.15		LMC 16-38	0.85	13.96	14.07	
LMC BW-34	1.27	13.96	13.61	yes	LMC 16-39	0.78	12.00	12.20	
LMC BW-35	0.78	13.48	13.68		LMC 16-40	0.82	14.02	14.17	
LMC BW-37	0.79	14.06	14.25		LMC 16-41	0.93	13.73	13.73	
LMC BW-38	1.10	13.38	13.16		LMC 16-42	1.07	13.52	13.34	
LMC BW-39	1.22	13.71	13.33		LMC 16-43	0.89	13.84	13.90	
LMC BW-40	1.01	13.77	13.67		LMC 16-44	0.95	14.09	14.07	
LMC BW-41	1.08	13.69	13.49		LMC 16-45	1.21	14.60	14.23	
LMC BW-42	1.24	13.79	13.46	yes	LMC 16-46	0.69	13.60	13.92	
LMC BW-44	1.11	14.12	13.79	yes	LMC 16-47	0.87	13.94	14.02	
LMC BW-47	1.15	13.44	13.15		LMC 16-48	1.08	13.79	13.59	
LMC BW-49	1.05	13.63	13.47		LMC 16-49	1.38	13.51	12.91	
LMC BW-51	1.27	14.34	13.89		LMC 17-1	1.08	13.35	13.15	
LMC BW-53	1.14	13.99	13.87	yes	LMC 17-2	1.18	13.92	13.59	
LMC BW-54	0.91	13.27	12.63	yes	LMC 17-3	1.39	14.39	13.78	
LMC BW-55	0.90	13.58	13.62		LMC 17-4	1.25	13.94	13.52	
LMC BW-57	1.21	13.53	13.16		LMC 17-5	1.18	14.20	13.87	
LMC BW-58	0.96	13.20	13.16		LMC 17-6	1.10	13.46	13.24	
LMC BW-65	1.04	13.46	13.32		LMC 17-8	1.22	13.96	13.58	
LMC BW-67	1.05	12.93	12.77		LMC 17-9	1.14	14.03	13.75	
LMC BW-69	1.25	13.53	13.11		LMC 17-10	0.91	13.16	13.19	
LMC BW-73	1.40	13.92	13.30		LMC 17-11	0.90	13.15	13.19	
LMC BW-74	2.25	14.05	12.30		LMC 17-11	1.15	13.89	13.60	
LMC BW-85	1.27	13.39	12.95	yes	LMC 17-12	1.12	13.97	13.72	
LMC BW-100	0.73	13.64	13.91		LMC 17-13	1.17	14.36	14.04	
LMC BW-103	1.07	13.82	13.64		LMC 17-14	1.11	14.50	14.26	
LMC BW-104	1.11	13.88	13.68	yes	LMC 17-15	1.04	13.79	13.65	
LMC BW-105	1.22	13.50	13.34	yes	LMC 17-16	0.77	12.53	12.75	
LMC BW-106	1.13	13.41	13.15		LMC 18-1	0.74	13.77	14.03	
LMC BW-108	1.10	14.06	13.98	yes	LMC 18-2	1.50	14.18	13.43	
LMC 16-1	1.15	13.93	13.64		LMC 18-3	0.99	15.45	15.37	
LMC 16-2	1.13	14.32	14.06		LMC 18-4	0.95	14.11	14.09	
LMC 16-3	1.10	13.57	13.35		LMC 18-5	1.21	13.66	13.29	
LMC 16-4	1.07	13.66	13.48		LMC 18-6	1.16	14.63	14.33	
LMC 16-5	0.98	13.54	13.48		LMC 18-7	1.18	13.74	13.41	
LMC 16-6	1.08	14.30	14.10		LMC 18-8	1.07	14.03	13.85	
LMC 16-7	0.89	14.03	14.09		LMC 18-9	1.23	13.49	13.09	
LMC 16-8	1.03	14.35	14.22		LMC 18-10	1.20	12.94	12.58	
LMC 16-9	0.89	13.83	13.89		LMC 18-11	0.80	13.31	13.49	
LMC 16-10	1.09	13.00	12.79		LMC 18-12	1.18	14.28	13.95	
LMC 16-11	1.21	13.94	13.57		LMC 18-13	1.17	13.68	13.36	
LMC 16-12	0.99	13.26	13.18		LMC 18-14	1.08	13.99	13.79	
LMC 16-13	1.23	13.77	13.37		LMC 18-15	1.11	13.91	13.67	
LMC 16-14	1.20	13.72	13.36		LMC 18-16	1.13	13.81	13.55	
LMC 16-15	0.64	13.80	14.19		LMC 18-17	1.31	14.06	13.56	
LMC 16-16	0.74	14.14	14.40		LMC 18-18	1.35	14.48	13.92	
LMC 16-17	1.45	13.93	13.24		LMC 18-19	0.85	14.16	14.27	
LMC 16-18	0.97	13.90	13.85		LMC 18-20	1.16	14.33	14.03	
LMC 16-19	0.73	14.60	14.87		LMC 19-1	1.01	13.62	13.52	
LMC 16-20	1.10	13.55	13.33		LMC 19-2	1.07	13.91	13.73	
LMC 16-21	0.67	13.80	14.15		LMC 19-3	0.79	14.01	14.20	
LMC 16-22	0.60	13.88	14.32		LMC 19-4	1.13	13.94	13.68	
LMC 16-23	1.24	13.93	13.52		LMC 19-5	0.91	13.45	13.48	
LMC 16-24	1.08	13.67	13.47		LMC 19-6	1.33	13.66	13.13	
LMC 16-25	1.09	14.28	14.07		LMC 19-7	1.05	14.32	14.16	
LMC 16-26	0.97	12.66	12.61		LMC 19-8	0.91	14.03	14.06	
LMC 16-27	1.07	13.22	13.04		LMC 20-1	1.28	14.20	13.70	yes
LMC 16-28	1.09	13.65	13.44		LMC 20-2	0.82	13.95	13.84	yes
LMC 16-29	1.22	14.00	13.62		LMC 20-3	1.09	15.42	14.68	yes
LMC 16-30	1.22	13.50	13.12		LMC 20-4	1.02	14.97	14.88	yes
LMC 16-31	1.12	13.74	13.49		LMC 20-5	0.94	13.76	13.58	yes
LMC 16-32	1.16	14.00	13.70		LMC 20-6	0.96	13.82	14.15	yes
LMC 16-33	1.03	13.37	13.24		LMC 20-7	0.85	14.27	14.47	yes
LMC 16-34	0.92	14.65	14.67		LMC 20-8	1.14	13.93	13.72	yes
LMC 16-35	1.04	13.82	13.68		LMC 20-9	1.24	13.85	13.70	yes
LMC 16-36	1.12	13.17	12.92		LMC 20-10	1.13	14.09	13.91	yes
LMC 16-37	1.36	14.43	13.86		LMC 20-11	0.92	13.52	13.42	yes

TABLE 2. (continued)

Star	$(R\ I)_0$	I_0	m_{bol}	JHK	Star	$(R\ I)_0$	I_0	m_{bol}	JHK
LMC 20-12	1.02	13.87	13.76	yes	LMC 24-1	1.02	13.89	13.77	
LMC 20-13	1.21	13.40	13.17	yes	LMC 24-2	1.36	13.50	12.93	
LMC 20-14	0.92	13.70	14.26	yes	LMC 24-3	0.92	13.62	13.64	
LMC 20-15	1.31	13.70	13.18	yes	LMC 24-4	0.63	14.75	15.15	
LMC 20-16	1.26	13.87	13.43		LMC 24-5	0.75	13.95	14.19	
LMC 20-17	0.94	13.77	13.67	yes	LMC 24-6	1.44	14.52	13.84	
LMC 20-18	0.85	14.70	14.85	yes	LMC 24-7	1.55	14.57	13.75	
LMC 20-19	1.26	14.89	13.84	yes	LMC 24-8	0.76	14.46	14.69	
LMC 20-20	1.22	13.89	13.55	yes	LMC 24-9	1.23	13.64	13.24	
LMC 20-21	0.89	13.44	13.50	yes	LMC 24-10	0.97	13.24	13.19	
LMC 20-24	1.04	14.79	14.79	yes	LMC 25-1	0.81	14.35	14.51	
LMC 20-25	0.94	13.90	13.89		LMC 25-2	1.04	13.07	12.93	
LMC 20-26	0.94	13.72	13.71		LMC 25-3	1.17	13.88	13.56	
LMC 20-27	1.44	13.67	12.99		LMC 25-4	1.14	13.69	13.41	
LMC 20-28	1.08	13.83	13.63		LMC 25-5	0.63	16.85	17.25	
LMC 20-29	0.80	13.46	13.64		LMC O-1	1.13	13.92	13.66	
LMC 20-30	1.06	14.17	14.00		LMC O-4	1.06	14.41	14.24	
LMC 20-31	1.29	13.96	13.48		LMC O-8	1.25	14.27	13.85	
LMC 21-2	0.93	13.57	13.57		LMC O-13	1.16	13.10	13.16	yes
LMC 21-3	0.79	14.52	14.71		LMC O-17	1.16	13.64	13.55	yes
LMC 21-4	0.87	14.44	14.52		LMC O-26	1.10	14.09	13.77	yes
LMC 21-5	0.99	13.54	13.46		LMC O-33	1.38	13.60	13.22	yes
LMC 21-6	0.91	13.77	13.80		LMC O-40	1.24	14.08	14.05	yes
LMC 21-7	0.97	13.18	13.13		LMC O-43	1.12	13.64	13.61	yes
LMC 21-8	1.05	13.98	13.82		LMC O-47	0.87	13.44	13.55	yes
LMC 21-9	0.83	14.50	14.64		LMC O-86	1.12	14.32	13.97	yes
LMC 21-10	1.09	13.62	13.41		LMC O-110	0.70	14.34	14.70	yes
LMC 21-11	0.98	14.18	14.12		LMC O-114	1.44	13.42	12.83	yes
LMC 21-12	1.41	14.21	13.57		LMC 27-1	1.04	14.40	14.26	
LMC 21-13	1.09	14.61	14.40		LMC 27-2	1.02	14.00	13.88	
LMC 21-14	1.18	14.01	13.68		LMC 27-3	0.95	14.08	14.06	
LMC 21-15	1.22	13.64	13.26		LMC 27-4	0.97	13.64	13.59	
LMC 21-16	1.14	14.05	13.77		LMC 27-5	1.05	13.78	13.62	
LMC 21-17	1.31	13.96	13.46		LMC 28-1	0.97	13.59	13.54	
LMC 21-18	1.11	14.21	13.97		LMC 28-2	0.82	13.70	13.85	
LMC 21-19	0.84	14.02	14.14		LMC 28-3	0.66	14.55	14.91	
LMC 21-20	1.30	13.91	13.42		LMC 28-4	0.73	14.06	14.33	
LMC 21-21	0.91	13.81	13.84		LMC 28-5	1.08	13.64	13.44	
LMC 21-22	1.18	14.06	13.73		LMC 28-6	0.91	13.07	13.10	
LMC 21-23	1.15	13.91	13.62		LMC 28-7	1.04	13.88	13.74	
LMC R-2	1.31	13.72	13.39	yes	LMC 28-8	0.85	14.51	14.62	
LMC R-12	1.35	13.78	12.75	yes	LMC 28-9	0.99	13.57	13.49	
LMC R-38	1.28	14.00	13.20	yes	LMC 28-10	1.07	14.16	13.98	
LMC R-45	1.02	12.90	12.74	yes	LMC 28-11	1.01	14.34	14.24	
LMC R-48	1.25	13.97	13.54	yes	LMC 28-12	1.06	13.81	13.64	
LMC R-53	1.33	13.92	13.35	yes	LMC 28-13	1.04	13.71	13.57	
LMC R-54	1.39	14.06	13.56	yes	LMC 28-14	0.79	13.84	14.03	
LMC 23-1	0.54	15.00	15.52		LMC 28-15	0.99	14.35	14.27	
LMC 23-2	1.05	14.33	14.17		LMC 28-16	1.19	13.47	13.13	
LMC 23-3	1.03	14.29	14.16		LMC 28-17	0.93	13.76	13.76	
LMC 23-4	0.97	13.50	13.45		LMC 28-18	1.32	13.66	13.14	
LMC 23-5	1.03	14.29	14.16		LMC 28-19	1.47	13.83	13.11	
LMC 23-6	1.19	13.76	13.42		LMC 28-20	0.74	14.80	15.06	
LMC 23-7	1.23	13.70	13.30		LMC 28-21	0.93	13.71	13.71	
LMC 23-8	1.16	13.58	13.28		LMC 28-22	0.96	13.52	13.48	
LMC 23-9	1.15	13.93	13.64		LMC 28-23	0.89	14.14	14.20	
LMC 23-10	1.15	13.82	13.53		LMC 28-24	1.10	13.77	13.55	
LMC 23-11	1.06	14.28	14.11		LMC 28-25	1.07	13.89	13.71	
LMC 23-12	0.79	13.84	14.03		LMC 28-26	1.19	13.67	13.33	
LMC 23-13	0.91	13.95	13.98		LMC 28-27	0.97	13.70	13.65	
LMC 23-14	0.85	14.17	14.28		LMC 28-28	0.75	14.55	14.79	
LMC 23-15	1.34	14.95	14.41		LMC 28-30	1.10	14.15	13.93	
LMC 23-16	1.11	13.77	13.53		LMC 28-31	1.74	16.87	15.80	
LMC 23-17	0.96	13.64	13.60		LMC 28-32	0.90	14.53	14.57	
LMC 23-18	0.96	14.29	14.25		LMC 28-33	0.93	14.37	14.37	
LMC 23-19	0.97	14.20	14.15		LMC 28-34	0.89	13.74	13.80	
LMC 23-20	1.08	13.70	13.50		LMC 28-35	0.95	13.85	13.83	

TABLE 2. (continued)

Star	$(R\ I)_0$	I_0	m_{bol}	JHK	Star	$(R\ I)_0$	I_0	m_{bol}	JHK
LMC 28-36	1.25	13.44	13.02		LMC 32-17	0.78	14.52	14.49	yes
LMC 28-37	1.10	13.89	13.67		LMC 32-18	1.01	14.13	13.35	yes
LMC 29-1	0.95	14.78	14.76		LMC 32-19	1.04	14.13	13.94	yes
LMC 29-2	1.04	13.35	13.21		LMC 32-20	0.97	14.11	14.29	yes
LMC 29-3	0.67	14.71	15.06		LMC 32-21	1.31	13.83	13.35	yes
LMC 29-4	0.93	14.47	14.47		LMC 32-22	1.41	15.36	13.86	yes
LMC 29-5	0.64	14.64	15.03		LMC 32-23	1.05	13.73	13.65	yes
LMC 29-6	1.30	15.17	14.68		LMC 32-24	0.99	14.21	13.89	yes
LMC 29-7	0.65	13.69	14.07		LMC 32-25	0.86	13.42	13.58	yes
LMC 29-8	1.04	13.66	13.52		LMC 33-1	0.77	13.37	13.39	yes
LMC 29-9	1.15	13.77	13.48		LMC 33-2	1.01	13.75	13.63	yes
LMC 29-10	1.37	14.68	14.10		LMC 33-3	1.16	14.63	13.40	yes
LMC 29-11	0.97	13.49	13.44		LMC 33-4	0.73	15.00	13.67	yes
LMC 29-12	1.20	13.76	13.40		LMC 33-5	1.14	14.39	14.12	yes
LMC 29-13	1.33	13.70	13.17		LMC 33-6	0.96	13.71	14.26	yes
LMC 30-1	1.31	13.61	13.11		LMC 33-7	1.17	13.61	13.69	yes
LMC 30-2	1.26	14.13	13.69		LMC 33-8	0.98	14.55	14.02	yes
LMC 30-3	1.13	15.58	15.32		LMC 33-9	1.14	13.40	13.59	yes
LMC 30-4	0.95	14.14	14.12		LMC 33-11	1.14	14.90	14.36	yes
LMC 30-5	1.06	13.83	13.66		LMC 33-12	1.85	14.43	13.63	yes
LMC 30-6	0.96	13.16	13.12		LMC 33-13	1.07	14.17	14.03	yes
LMC 30-7	0.91	12.59	12.62		LMC 33-14	0.78	14.11	14.48	yes
LMC 30-8	0.88	13.47	13.54		LMC 33-15	0.97	13.52	13.58	yes
LMC 30-9	1.40	13.49	12.87		LMC 33-16	1.26	13.82	13.72	yes
LMC 30-10	0.97	13.69	13.64		LMC 33-17	1.08	13.86	13.85	yes
LMC 30-11	0.91	13.54	13.57		LMC 33-18	0.91	13.66	13.82	yes
LMC 30-12	1.09	13.83	13.62		LMC 33-19	0.79	14.03	14.31	yes
LMC 30-13	0.92	13.82	13.84		LMC 33-20	1.20	13.68	13.55	yes
LMC 30-14	1.38	14.02	13.42		LMC 33-21	1.20	13.41	13.20	yes
LMC 30-15	1.06	14.24	14.07		LMC 33-22	1.17	13.66	13.63	yes
LMC 30-16	1.10	13.80	13.58		LMC 33-23	1.60	14.41	13.82	yes
LMC 30-17	0.97	14.37	14.32		LMC 33-24	1.19	13.45	13.32	yes
LMC 30-18	0.88	14.10	14.17		LMC 33-25	1.41	15.46	14.82	
LMC 30-19	0.89	14.24	14.30		LMC 33-26	1.35	13.95	13.39	
LMC 30-20	1.22	14.06	13.68		LMC 33-27	0.90	13.95	13.99	
LMC 30-21	1.09	14.07	13.86		LMC 33-28	0.94	14.35	14.34	
LMC 30-22	0.99	13.88	13.80		LMC 33-29	0.81	13.87	14.03	
LMC 30-23	0.93	12.58	12.58		LMC 33-30	1.21	13.72	13.35	
LMC 30-24	1.01	13.78	13.68		LMC 33-31	1.28	14.07	13.61	
LMC 30-25	1.02	14.25	14.13		LMC 33-32	0.76	14.50	14.73	
LMC 30-26	1.47	14.30	13.58		LMC 33-33	1.11	13.94	13.70	
LMC 30-27	0.82	14.02	14.17		LMC 33-34	1.45	14.55	13.86	
LMC 30-29	0.86	13.58	13.68		LMC 33-35	0.96	13.62	13.58	
LMC 30-30	1.05	13.52	13.36		LMC 33-36	0.98	13.63	13.57	
LMC 30-31	1.05	13.19	13.03		LMC 33-37	1.40	13.99	13.37	
LMC 30-32	1.03	13.89	13.76		LMC 33-38	0.86	14.16	14.26	
LMC 30-33	1.26	14.01	13.57		LMC 33-39	0.99	13.53	13.45	
LMC 31-1	1.39	13.77	13.16		LMC 33-40	1.16	13.95	13.65	
LMC 31-2	1.26	13.36	12.92		LMC 33-41	1.18	13.41	13.08	
LMC 31-3	1.01	13.42	13.32		LMC 33-42	1.19	13.61	13.27	
LMC 31-4	1.21	14.03	13.66		LMC 33-43	1.26	13.88	13.44	
LMC 31-5	0.78	13.79	13.99		LMC 33-44	1.26	15.02	14.58	
LMC 32-1	1.37	14.43	13.42	yes	LMC 33-45	0.98	14.02	13.96	
LMC 32-2	1.46	14.98	13.97	yes	LMC 33-46	1.39	13.82	13.21	
LMC 32-3	1.32	14.19	13.64	yes	LMC 33-47	0.93	13.88	13.88	
LMC 32-4	1.27	14.55	14.12	yes	LMC 33-48	1.35	14.07	13.51	
LMC 32-5	1.09	14.63	14.19	yes	LMC 33-49	0.90	13.85	13.89	
LMC 32-6	0.94	14.57	14.65	yes	LMC 33-50	0.89	14.53	14.59	
LMC 32-7	1.17	13.80	13.58	yes	LMC 33-51	1.24	15.00	14.59	
LMC 32-8	1.06	14.28	14.11	yes	LMC 33-52	0.97	13.40	13.35	
LMC 32-10	0.93	13.69	13.41	yes	LMC 33-53	1.28	14.09	13.63	
LMC 32-11	0.71	13.34	13.39	yes	LMC 33-54	0.72	13.92	14.20	
LMC 32-12	1.03	14.53	14.95	yes	LMC 33-55	1.04	13.86	13.72	
LMC 32-13	1.01	14.20	14.24	yes	LMC 33-56	1.26	13.98	13.54	
LMC 32-14	0.98	14.27	14.06	yes	LMC 33-57	1.06	13.70	13.53	
LMC 32-15	1.20	14.38	14.14	yes	LMC 33-58	1.41	13.43	12.79	
LMC 32-16	1.08	14.13	14.11	yes	LMC 33-59	1.20	13.90	13.54	

TABLE 2. (continued)

Star	$(R\ I)_0$	I_0	m_{bol}	JHK	Star	$(R\ I)_0$	I_0	m_{bol}	JHK
LMC 33-60	1.02	13.79	13.67		LMC 35-18	1.04	13.85	13.71	
LMC 33-61	1.07	13.64	13.46		LMC 35-19	0.86	13.80	13.90	
LMC 33-62	1.10	13.96	13.74		LMC 35-20	0.84	13.68	13.80	
LMC 33-63	1.19	13.97	13.63		LMC 35-21	1.07	14.51	14.33	
LMC 33-64	1.03	13.73	13.60		LMC 35-22	1.08	14.10	13.90	
LMC 33-65	1.48	14.40	13.67		LMC 35-23	1.01	13.90	13.80	
LMC 33-66	1.18	14.18	13.85		LMC 35-24	1.23	13.72	13.32	
LMC 33-67	1.02	13.78	13.66		LMC 36-1	1.02	14.16	14.04	
LMC 33-68	1.18	14.54	14.21		LMC 36-2	1.30	14.19	13.70	
LMC 33-69	1.42	14.38	13.73		LMC 36-3	0.89	13.48	13.54	
LMC 33-70	0.89	13.65	13.71		LMC 36-5	0.88	14.00	14.07	
LMC 33-71	1.03	13.59	13.46		LMC 36-6	0.86	14.50	14.60	
LMC 33-72	1.02	14.11	13.99		LMC 36-7	1.30	14.03	13.54	
LMC 33-73	1.00	13.90	13.81		LMC 36-8	1.26	13.91	13.47	
LMC 33-74	1.01	14.19	14.09		LMC 36-11	1.03	14.36	14.23	
LMC 33-75	0.96	14.39	14.35		LMC 36-12	1.26	14.01	13.57	
LMC 33-76	0.65	14.74	15.12		LMC 36-13	0.88	14.19	14.26	
LMC 33-77	1.04	13.97	13.83		LMC 36-14	0.99	13.87	13.79	
LMC 33-78	0.80	14.40	14.58		LMC 36-15	1.33	13.82	13.29	
LMC 33-79	0.98	15.54	15.48		LMC 36-16	1.21	13.72	13.35	
LMC 33-80	1.22	14.31	13.93		LMC 36-17	1.32	15.25	14.73	
LMC 33-81	1.05	13.74	13.58		LMC 36-18	0.78	13.99	14.19	
LMC 34-1	0.76	13.81	14.04		LMC 36-19	1.22	13.99	13.61	
LMC 34-2	1.17	13.63	13.31		LMC 36-20	0.95	13.50	13.48	
LMC 34-3	1.01	13.60	13.50		LMC 36-21	1.03	14.61	14.48	
LMC 34-4	1.27	14.47	14.02		LMC 36-22	1.36	13.88	13.31	
LMC 34-5	1.26	14.09	13.65		LMC 36-23	1.36	14.10	13.53	
LMC 34-6	1.14	13.95	13.67		LMC 37-1	1.12	14.12	13.68	yes
LMC 34-7	1.27	13.81	13.36		LMC 37-2	1.24	13.58	13.13	yes
LMC 34-8	0.85	14.34	14.45		LMC 37-3	0.88	14.02	13.75	yes
LMC 34-9	1.19	13.35	13.01		LMC 37-4	1.26	14.11	13.92	yes
LMC 34-10	1.07	13.93	13.75		LMC 37-5	1.30	15.17	14.14	yes
LMC 34-11	1.00	13.53	13.44		LMC 37-6	1.47	14.40	13.90	yes
LMC 34-12	1.10	14.31	14.09		LMC 37-7	1.08	13.63	13.41	yes
LMC 34-14	0.92	13.52	13.54		LMC 37-8	1.01	14.63	14.46	yes
LMC 34-16	1.38	13.78	13.18		LMC 37-9	0.92	13.70	13.82	yes
LMC 34-17	1.15	14.06	13.77		LMC 37-10	1.28	14.35	14.06	yes
LMC 34-18	1.00	14.19	14.10		LMC 37-11	1.09	14.77	14.41	yes
LMC 34-19	1.01	14.32	14.22		LMC 37-12	0.90	14.34	14.17	yes
LMC 34-20	0.93	13.70	13.70		LMC 37-13	1.21	13.99	13.75	yes
LMC 34-21	1.31	14.26	13.76		LMC 37-14	1.22	13.99	13.65	yes
LMC 34-22	0.89	14.57	14.63		LMC 37-15	1.81	15.45	14.28	
LMC 34-23	1.07	13.90	13.72		LMC 37-16	1.14	14.40	13.82	yes
LMC 34-24	0.98	14.34	14.28		LMC 37-17	0.86	14.32	14.37	yes
LMC 34-25	1.45	14.06	13.37		LMC 37-18	0.91	14.32	14.22	yes
LMC 34-26	1.21	14.03	13.66		LMC 37-19	1.01	14.36	13.93	yes
LMC 34-27	0.94	13.79	13.78		LMC 37-20	1.22	14.45	14.04	yes
LMC 34-28	1.11	13.72	13.48		LMC 37-21	1.27	13.77	13.17	yes
LMC 34-29	1.04	14.18	14.04		LMC 37-22	1.06	14.21	14.21	yes
LMC 34-30	0.98	13.38	13.32		LMC 37-23	0.88	14.02	13.80	yes
LMC 35-1	0.93	14.01	14.01		LMC 37-25	0.73	15.28	15.84	yes
LMC 35-2	0.96	13.62	13.58		LMC 37-26	1.12	13.89	13.60	yes
LMC 35-3	1.17	13.32	13.00		LMC 37-27	1.13	14.13	13.87	
LMC 35-4	0.88	13.96	14.03		LMC 37-28	0.94	13.70	13.69	
LMC 35-5	1.02	14.19	14.07		LMC 37-29	0.89	14.01	14.07	
LMC 35-6	1.29	13.90	13.42		LMC 37-30	1.38	14.27	13.67	
LMC 35-7	0.78	13.90	14.10		LMC 37-31	1.13	13.81	13.55	
LMC 35-8	1.37	14.30	13.72		LMC 37-32	1.18	13.51	13.18	
LMC 35-9	0.98	13.88	13.82		LMC 37-33	0.94	13.72	13.71	
LMC 35-10	1.14	14.06	13.78		LMC 37-34	1.07	13.92	13.74	
LMC 35-11	1.30	13.60	13.11		LMC 37-35	1.12	14.26	14.01	
LMC 35-12	0.97	12.87	12.82		LMC 37-36	0.98	13.33	13.27	
LMC 35-13	0.80	14.20	14.38		LMC 37-37	0.64	15.07	15.46	
LMC 35-14	0.95	13.34	13.32		LMC 37-38	1.08	13.99	13.79	
LMC 35-15	0.98	14.12	14.06		LMC 37-39	0.85	13.66	13.77	
LMC 35-16	1.47	14.35	13.63		LMC 37-40	1.12	14.31	14.06	
LMC 35-17	1.01	13.78	13.68		LMC 37-41	1.16	13.95	13.65	

TABLE 2. (continued)

Star	$(R\ I)_0$	I_0	m_{bol}	JHK	Star	$(R\ I)_0$	I_0	m_{bol}	JHK
LMC 37-42	1.28	13.75	13.29		LMC 42-23	0.89	13.80	13.86	
LMC 37-43	1.21	13.65	13.28		LMC 42-24	1.16	14.01	13.71	
LMC 37-44	0.92	14.39	14.41		LMC 42-25	0.94	13.25	13.24	
LMC 37-45	0.87	14.86	14.94		LMC 42-26	1.07	13.81	13.63	
LMC 38-1	1.29	14.51	13.93	yes	LMC 42-27	1.01	14.14	14.04	
LMC 38-2	1.07	13.76	13.56	yes	LMC 42-28	0.79	13.65	13.84	
LMC 38-3	1.45	14.06	13.52	yes	LMC 42-30	1.07	14.00	13.82	
LMC 38-4	0.84	13.62	13.72	yes	LMC 42-31	1.18	13.82	13.49	
LMC 38-5	0.90	12.85	12.61	yes	LMC 42-32	0.34	14.09	14.88	
LMC 38-6	1.21	14.48	14.24	yes	LMC 42-33	1.06	14.59	14.42	
LMC 38-7	1.15	13.93	13.47	yes	LMC 42-34	1.04	13.71	13.57	
LMC 38-8	1.14	14.11	13.84	yes	LMC 43-1	0.73	14.27	14.54	
LMC 38-9	1.13	14.45	14.14	yes	LMC 43-2	1.03	13.91	13.78	
LMC 38-10	1.29	13.42	12.63	yes	LMC 43-3	1.41	13.87	13.23	
LMC 38-11	1.04	14.28	13.49	yes	LMC 43-4	1.02	13.64	13.52	
LMC 38-12	0.91	14.32	14.13	yes	LMC 43-5	0.90	13.75	13.79	
LMC 38-13	1.13	14.13	14.31	yes	LMC 43-6	1.44	14.02	13.34	
LMC 38-14	0.94	14.28	14.22	yes	LMC 43-7	1.02	14.41	14.29	
LMC 38-15	1.02	14.15	14.28	yes	LMC 43-10	1.00	14.05	13.96	
LMC 38-16	0.97	13.51	13.05	yes	LMC 43-11	0.71	14.51	14.81	
LMC 38-17	0.93	13.59	13.68	yes	LMC 43-12	1.01	14.02	13.92	
LMC 38-18	0.98	13.96	13.90	yes	LMC 43-13	1.34	13.87	13.33	
LMC 38-19	1.06	13.57	13.47	yes	LMC 43-14	0.90	13.52	13.56	
LMC 38-20	1.20	14.38	13.93	yes	LMC 43-15	1.17	14.24	13.92	
LMC 38-21	1.35	13.82	13.48	yes	LMC 43-16	1.17	13.65	13.33	
LMC 38-22	0.98	14.33	14.41	yes	LMC 43-17	0.52	15.35	15.90	
LMC 39-1	1.01	13.64	13.54		LMC 43-18	0.92	14.20	14.22	
LMC 39-2	0.83	13.82	13.96		LMC 43-19	1.08	13.89	13.69	
LMC 39-3	1.16	14.98	14.68		LMC 43-20	1.27	13.40	12.95	
LMC 39-4	1.31	13.68	13.18		LMC 43-22	1.11	13.84	13.60	
LMC 39-5	0.89	13.64	13.70		LMC 43-23	1.07	13.65	13.47	
LMC 39-6	1.01	14.14	14.04		LMC 44-1	1.34	13.82	13.28	
LMC 39-8	0.77	14.26	14.48		LMC 44-2	1.01	13.47	13.37	
LMC 39-9	1.27	13.79	13.34		LMC 44-3	1.40	13.67	13.05	
LMC 40-1	1.16	14.46	14.16		LMC 44-4	1.18	13.33	13.00	
LMC 40-2	1.48	14.13	13.40		LMC 44-5	0.84	13.42	13.54	
LMC 40-3	1.23	13.68	13.28		LMC 44-6	1.11	13.96	13.72	
LMC 40-4	1.00	13.42	13.33		LMC 44-7	1.03	14.25	14.12	
LMC 40-5	1.14	14.14	13.86		LMC 44-8	0.62	14.12	14.54	
LMC 40-6	1.03	13.88	13.75		LMC 45-1	1.04	13.73	13.59	
LMC 40-7	1.13	14.03	13.77		LMC 45-2	1.19	13.49	13.15	
LMC 40-8	0.90	14.10	14.14		LMC 45-4	1.05	13.47	13.31	
LMC 41-1	0.62	14.90	15.32		LMC 45-5	1.07	13.41	13.23	
LMC 41-2	1.08	13.63	13.43		LMC 45-6	0.98	13.71	13.65	
LMC 41-3	1.18	13.81	13.48		LMC 46-1	0.96	13.60	13.56	
LMC 41-4	1.42	14.02	13.37		LMC 46-2	0.72	14.47	14.75	
LMC 42-1	1.42	14.24	13.59		LMC 46-3	1.21	13.69	13.32	
LMC 42-3	1.19	13.67	13.33		LMC 46-5	1.14	13.89	13.61	
LMC 42-4	0.68	14.11	14.45		LMC 46-6	1.01	13.41	13.31	
LMC 42-5	0.90	14.92	14.96		LMC 46-7	1.29	13.58	13.10	
LMC 42-6	1.11	13.84	13.60		LMC 46-8	1.19	13.67	13.33	
LMC 42-7	1.05	14.71	14.55		LMC 46-9	1.17	14.59	14.27	
LMC 42-8	1.21	14.38	14.01		LMC 46-10	1.32	13.80	13.28	
LMC 42-9	1.08	13.87	13.67		LMC 47-1	1.21	13.79	13.42	
LMC 42-10	1.28	14.00	13.54		LMC 48-1	0.83	14.21	14.35	
LMC 42-11	1.40	13.69	13.07		LMC 48-2	0.97	13.87	13.82	
LMC 42-12	1.15	12.92	12.63		LMC 48-3	1.17	13.72	13.40	
LMC 42-13	0.99	14.28	14.20		LMC 48-4	0.91	13.65	13.68	
LMC 42-14	0.90	14.36	14.40		LMC 49-1	1.32	13.95	13.43	
LMC 42-15	0.98	13.62	13.56		LMC 49-2	1.01	14.16	14.06	
LMC 42-16	1.12	14.02	13.77		LMC 49-3	0.95	14.07	14.05	
LMC 42-17	1.05	14.02	13.86		LMC 49-4	0.81	14.15	14.31	
LMC 42-18	0.70	14.70	15.01		LMC 50-1	0.90	14.23	14.27	
LMC 42-19	1.07	14.17	13.99		LMC 50-2	0.88	14.91	14.98	
LMC 42-20	0.78	14.73	14.93		LMC 50-3	0.69	14.20	14.52	
LMC 42-21	0.89	14.38	14.44		LMC 50-4	0.94	13.81	13.80	
LMC 42-22	1.43	14.35	13.69		LMC 50-5	1.29	14.09	13.61	

TABLE 2. (continued)

Star	$(R\ I)_0$	I_0	m_{bol}	JHK
LMC 50-6	0.72	14.92	15.20	
LMC 51-1	1.33	13.84	13.31	
LMC 51-2	1.34	14.14	13.60	
LMC 51-3	0.86	14.00	14.10	
LMC 51-4	1.28	13.57	13.11	
LMC 51-5	1.19	13.69	13.35	
LMC 51-6	0.86	13.64	13.74	
LMC 51-7	1.12	13.50	13.25	
LMC 51-8	1.17	13.55	13.23	
LMC 52-1	0.90	14.08	14.12	
LMC 52-2	0.97	13.81	13.76	
LMC 52-3	0.91	13.57	13.60	
LMC 52-4	1.20	13.66	13.30	
LMC 52-5	0.91	14.19	14.22	
LMC 52-6	0.92	13.35	13.37	
LMC 52-7	1.00	14.35	14.26	
LMC 52-8	1.32	13.68	13.16	
LMC 52-9	1.00	14.38	14.29	
WORC 227	0.98	13.86	13.80	
WORC 228	1.48	14.40	13.67	
WORC 229	1.13	14.33	14.07	
WORC 232	0.96	13.50	13.47	
WORC 233	1.06	13.55	13.38	
WORC 234	1.14	13.79	13.52	
WORC 235	0.88	13.73	13.80	
WORC 238	1.13	13.95	13.69	
WORC 240	0.79	14.77	14.96	
WORC 244	0.96	13.91	13.88	
WORC 246	1.15	13.79	13.50	
WORC 250	0.88	13.37	13.44	
WORC 253	0.82	13.46	13.61	
WORC 256	0.78	14.36	14.57	
WORC 259	1.26	13.54	13.11	
WORC 263	1.30	13.86	13.37	
WORC 266	1.44	13.96	13.29	
WORC 270	0.85	13.78	13.89	
WORC 273	1.15	13.78	13.49	
WORC 276	1.27	13.57	13.12	
WORC 278	1.11	12.82	12.59	
WORC 282	1.02	13.54	13.43	
WORC 283	1.25	13.71	13.29	
WORC 285	1.29	14.28	13.81	
WORC 288	1.18	13.66	13.33	
WORC 289	1.03	13.84	13.71	
WORC 290	1.41	14.72	14.09	
WORC 291	0.97	13.80	13.75	
WORC 292	1.04	13.25	13.11	
WORC 293	1.07	13.61	13.43	
WORC 295	1.18	13.50	13.17	
WORC 297	0.93	13.94	13.95	
WORC 298	0.96	13.44	13.41	
WORC 299	1.04	14.00	13.86	
WORC 302	1.01	13.78	13.68	

found by BM or BMB, the stars that were observed were selected in a random fashion without regard to brightness or color. Other observational techniques and uncertainties are as described by Frogel & Blanco (1990).

2.4 Reddening Corrections

Table 1 lists the $E(B-V)$ values adopted for the LMC fields in which we observed C stars. If an $E(B-V)$ value for a cluster within or close to a field was available from the literature, that value was adopted for the field; if not, an educated guess was made based on the work of Brunet (1975) and Bessell (1991). It should be noted, though, that none of the results discussed in this paper depends critically on the adopted reddening. To obtain the reddening corrected data in Tables 2 and 3 we used the reddening law for C stars given in CFPE. From CFPE we have $A_{V,0}=3.2\ E(B-V)_0$; $A_{V,0}=1$ corresponds to 0.77, 0.60, 0.265, 0.155, and 0.090 mag of extinction at R(kc), I(kc), J, H, and K, respectively.

2.5 Bolometric Magnitudes

2.5.1 Stars with RI and JHK photometry

The bolometric magnitudes (m_{bol}) for the stars with JHK photometry were calculated using the relation between the bolometric correction for the K magnitude (BC_K) and the $(J-K)_0$ color given by Frogel *et al.* (1980, hereafter FPC). This relation was derived by FPC starting from the multicolor photometry of Mendoza & Johnson (1965) for galactic C stars. An empirical fit to the data shown in Fig. 2 of FPC gives

$$BC_K=1.09+1.69(J-K)+0.12(J-K)^2-0.34(J-K)^3+0.07(J-K)^4. \quad (1)$$

The sign convention adopted is such that $m_{bol}=K_0+BC_K$. The JHK colors of the galactic C stars and those in the LMC field are similar enough so that Eq. (1), derived from observations of the former stars, should apply to the latter ones as well (CFPE). This is indeed the case that was verified by direct integration of the energy distributions for the stars in the present sample with $RIJHK$ data. The bolometric corrections derived are insensitive to estimates for the UBV colors. The resulting values for m_{bol} are given in Table 3.

2.5.2 Stars with RI photometry only

With bolometric magnitudes calculated for stars with JHK photometry, we can formulate a method to obtain m_{bol} for the majority of the stars in our sample with only RI data. Figure 1 shows (I_0-m_{bol}) as a function of $(R-I)_0$ for stars with complete $RIJHK$ data. An unbiased least-squares fit to these data (solid line in Fig. 1) yields the relation:

$$I_0-m_{bol}=1.33(\pm0.13)\times(R-I)_0-1.24(\pm0.14). \quad (2)$$

The predicted uncertainty in I_0-m_{bol} is ±0.34.[4] Equation (2), then, supersedes the relation derived with an identical procedure by CFPE but based on only 34 LMC C stars with photographic rather than photometric $(R-I)$ colors. Table 2(a) gives the m_{bol} values calculated with Eq. (2) for the 727 C stars in our sample with only RI photometry. For stars with JHK data, the values of m_{bol} in this table merely repeat the values from Table 3 based on Eq. (1). Finally, Fig. 1 also show the mean relation for the SMC C stars derived by CFPE (dotted line); the agreement between it and that given by Eq. (2) is good.

[4]Before accurate absolute bolometric magnitudes were known for C stars based on near-IR observations in the Clouds, the I_0 magnitude alone was often used to predict m_{bol}. From the same sample of C stars used to derive Eq. (2), we obtain $m_{bol}=0.63(\pm0.05)\times I_0+4.96(\pm0.76)$. Although the formal uncertainty in m_{bol} is ±0.38, comparison with Eq. (2) shows that the lack of a color term will introduce a systematic error of nearly one magnitude in m_{bol} over the relevant color range.

TABLE 3. Reddening corrected photometry for LMC carbon stars with *JHK* data.

Star	I_0	$(R-I)_0$	K_0	$(J-K)_0$	$(H-K)_0$	m_{bol}	Star	I_0	$(R-I)_0$	K_0	$(J-K)_0$	$(H-K)_0$	m_{bol}
LMC 09-1	—	—	10.53	2.31	1.01	13.85	LMC 20-2	13.95	0.82	10.76	1.51	0.51	13.84
LMC 09-2	13.69	1.28	11.21	1.32	0.41	14.15	LMC 20-3	15.42	1.09	11.43	1.89	0.83	14.68
LMC 09-3	13.96	1.02	11.32	1.23	0.35	14.18	LMC 20-4	14.97	1.02	11.88	1.39	0.44	14.88
LMC 09-4	13.92	0.89	11.41	1.04	0.26	14.08	LMC 20-5	13.76	0.94	10.60	1.37	0.43	13.58
LMC 09-5	14.26	0.82	11.66	1.18	0.34	14.48	LMC 20-6	13.82	0.96	11.11	1.45	0.48	14.15
LMC 09-6	14.23	0.95	10.95	1.52	0.51	14.04	LMC 20-7	14.27	0.85	11.18	2.06	0.85	14.47
LMC 09-7	14.49	0.95	11.50	1.62	0.56	14.65	LMC 20-8	13.93	1.14	10.54	1.69	0.60	13.72
LMC 09-8	13.68	1.39	9.89	2.01	0.84	13.17	LMC 20-9	13.85	1.24	10.55	1.63	0.57	13.70
LMC 09-9	13.59	1.03	10.47	1.60	0.59	13.60	LMC 20-10	14.09	1.13	10.88	1.44	0.46	13.91
LMC 09-10	13.84	1.08	10.58	1.47	0.48	13.64	LMC 20-11	13.52	0.92	10.50	1.29	0.35	13.42
LMC 09-11	13.77	1.05	10.58	1.41	0.44	13.59	LMC 20-12	13.87	1.02	10.62	1.61	0.62	13.76
LMC 09-12	13.80	1.05	10.55	1.59	0.54	13.68	LMC 20-13	13.40	1.21	9.97	1.73	0.64	13.17
LMC 09-13	13.54	1.05	10.63	1.47	0.51	13.69	LMC 20-14	13.70	0.92	11.18	1.50	0.49	14.26
LMC 09-14	13.76	0.86	10.70	1.35	0.39	13.67	LMC 20-15	13.70	1.31	9.96	1.80	0.70	13.18
LMC 09-15	13.56	0.48	10.68	1.38	0.45	13.67	LMC 20-17	13.77	0.94	10.49	1.68	0.61	13.67
LMC 09-16	13.89	1.00	10.87	1.38	0.42	13.86	LMC 20-18	14.70	0.85	11.92	1.30	0.40	14.85
LMC 09-17	13.84	1.07	10.72	1.45	0.47	13.76	LMC 20-19	14.89	1.26	10.70	1.61	0.59	13.84
LMC 09-18	13.20	0.92	10.43	1.24	0.36	13.30	LMC 20-20	13.89	1.22	10.40	1.62	0.60	13.55
LMC 09-19	14.28	1.32	9.69	1.86	0.73	12.93	LMC 20-21	13.44	0.89	10.49	1.40	0.48	13.50
LMC 09-20	14.24	1.25	10.60	1.70	0.64	13.78	LMC 20-22	—	—	11.31	1.37	0.42	14.29
LMC 09-21	14.65	0.89	11.75	1.14	0.30	14.53	LMC 20-23	—	—	11.85	1.03	0.2	14.51
LMC 09-22	13.44	0.59	11.64	1.49	0.53	14.71	LMC 20-24	14.79	1.04	11.65	1.61	0.60	14.79
LMC 09-23	14.15	1.07	11.13	1.43	0.47	14.16	LMC R-2	13.72	1.31	10.19	1.73	0.67	13.39
LMC 09-24	—	—	11.21	1.66	0.62	14.38	LMC R-12	13.78	1.35	9.56	1.72	0.68	12.75
LMC 09-25	14.19	1.45	10.64	1.83	0.70	13.87	LMC R-38	14.00	1.28	10.03	1.67	0.63	13.20
LMC 09-26	13.95	0.90	11.57	2.10	0.88	14.87	LMC R-45	12.90	1.02	9.73	1.41	0.48	12.74
LMC 09-27	14.46	1.20	11.16	1.80	0.67	14.38	LMC R-48	13.97	1.25	10.41	1.60	0.59	13.54
LMC 09-28	13.65	1.27	10.56	1.71	0.66	13.75	LMC R-53	13.92	1.33	10.07	1.98	0.79	13.35
LMC 09-29	13.35	0.99	10.59	1.28	0.38	13.50	LMC R-54	14.06	1.39	10.31	1.88	0.79	13.56
LMC 09-30	13.68	1.19	10.90	1.62	0.60	14.05	LMC O-13	13.10	1.16	9.98	1.69	0.65	13.16
LMC 09-31	13.70	0.91	11.34	1.19	0.32	14.17	LMC O-17	13.64	1.16	10.42	1.60	0.58	13.55
LMC 09-32	14.01	1.15	11.06	1.46	0.47	14.11	LMC O-26	14.09	1.10	10.69	1.50	0.50	13.77
LMC 12-1	13.91	0.94	11.00	1.39	0.42	14.00	LMC O-33	13.60	1.38	9.99	1.83	0.70	13.22
LMC 12-2	14.76	1.19	10.46	2.13	0.92	13.76	LMC O-40	14.08	1.24	10.83	1.79	0.68	14.05
LMC 12-3	13.72	0.89	10.71	1.38	0.42	13.70	LMC O-43	13.64	1.12	10.55	1.48	0.50	13.61
LMC 12-4	14.33	0.80	11.99	1.28	0.38	14.90	LMC O-47	13.44	0.87	10.75	1.16	0.30	13.55
LMC 12-5	13.09	1.09	9.76	1.95	0.75	13.03	LMC O-86	14.32	1.12	10.65	2.38	1.07	13.97
LMC 12-6	14.40	1.09	11.01	1.60	0.59	14.14	LMC O-110	14.34	0.70	11.91	1.15	0.32	14.70
LMC 12-7	13.45	1.00	10.69	1.61	0.57	13.83	LMC O-114	13.42	1.44	9.63	1.73	0.66	12.83
LMC 12-8	15.64	1.50	10.63	2.42	1.07	13.95	LMC 32-1	14.43	1.37	10.16	1.90	0.72	13.42
LMC 12-9	13.76	1.09	10.49	1.44	0.47	13.52	LMC 32-2	14.98	1.46	10.70	1.97	0.73	13.97
LMC 12-10	13.97	1.25	10.50	1.64	0.59	13.66	LMC 32-3	14.19	1.32	10.39	1.88	0.68	13.64
LMC 12-11	14.11	0.92	11.03	1.38	0.43	14.02	LMC 32-4	14.55	1.27	10.93	1.72	0.62	14.12
LMC 12-12	13.66	1.20	10.24	1.56	0.55	13.35	LMC 32-5	14.63	1.09	11.03	1.64	0.56	14.19
LMC 12-13	14.13	1.09	10.27	2.06	0.87	13.56	LMC 32-6	14.57	0.94	11.75	1.27	0.41	14.65
LMC 12-14	13.10	1.06	9.77	1.49	0.52	12.84	LMC 32-7	13.80	1.17	10.42	1.65	0.62	13.58
LMC 12-15	13.99	1.21	10.69	1.47	0.50	13.75	LMC 32-8	14.28	1.06	11.02	1.52	0.52	14.11
LMC 12-16	14.49	1.15	11.32	1.34	0.44	14.28	LMC 32-9	—	—	10.16	3.51	1.64	12.76
LMC 12-17	14.28	1.32	9.80	2.01	0.85	13.08	LMC 32-9	—	—	10.17	3.44	1.63	12.85
LMC 12-18	13.18	0.94	10.20	1.18	0.32	13.02	LMC 32-10	13.69	0.93	10.27	1.61	0.56	13.41
LMC 12-19	12.64	0.61	10.17	0.91	0.22	12.68	LMC 32-11	13.34	0.71	10.57	1.18	0.39	13.39
LMC BW-1	16.14	1.47	10.75	1.66	0.57	13.92	LMC 32-12	14.53	1.03	11.63	2.26	1.01	14.95
LMC BW-3	13.47	1.01	10.21	1.44	0.48	13.24	LMC 32-13	14.20	1.01	11.31	1.31	0.39	14.24
LMC BW-9	14.59	0.99	11.58	1.44	0.51	14.61	LMC 32-14	14.27	0.98	11.26	1.16	0.27	14.06
LMC BW-11	13.61	1.20	10.06	1.51	0.53	13.14	LMC 32-15	14.38	1.20	11.12	1.42	0.47	14.14
LMC BW-19	13.90	0.94	11.15	1.08	0.23	13.86	LMC 32-16	14.13	1.08	11.08	1.44	0.49	14.11
LMC BW-21	13.78	1.12	10.63	1.50	0.50	13.71	LMC 32-17	14.52	0.78	11.87	1.00	0.24	14.49
LMC BW-24	14.37	1.32	10.36	1.51	0.51	13.44	LMC 32-18	14.13	1.01	10.30	1.46	0.54	13.35
LMC BW-25	13.45	1.25	9.94	1.67	0.62	13.11	LMC 32-19	14.13	1.04	10.71	1.83	0.68	13.94
LMC BW-34	13.96	1.27	10.38	1.81	0.74	13.61	LMC 32-20	14.11	0.97	11.26	1.43	0.47	14.29
LMC BW-42	13.79	1.24	10.31	1.62	0.59	13.46	LMC 32-21	13.83	1.31	10.16	1.72	0.64	13.35
LMC BW-44	14.12	1.11	10.68	1.55	0.55	13.79	LMC 32-22	15.36	1.41	10.54	2.36	1.03	13.86
LMC BW-53	13.99	1.14	10.68	1.71	0.62	13.87	LMC 32-23	13.73	1.05	10.52	1.59	0.55	13.65
LMC BW-54	13.27	0.91	9.66	1.35	0.43	12.63	LMC 32-24	14.21	0.99	10.85	1.45	0.48	13.89
LMC BW-85	13.39	1.27	9.73	1.80	0.69	12.95	LMC 32-25	13.42	0.86	10.75	1.19	0.30	13.58
LMC BW-104	13.88	1.11	10.67	1.41	0.43	13.68	LMC 33-1	13.37	0.77	10.33	1.47	0.48	13.39
LMC BW-105	13.50	1.22	10.17	1.67	0.62	13.34	LMC 33-2	13.75	1.01	10.53	1.54	0.54	13.63
LMC BW-108	14.06	1.10	10.89	1.52	0.53	13.98	LMC 33-3	14.63	1.16	10.14	1.90	0.75	13.40
LMC 20-1	14.20	1.28	10.50	1.74	0.65	13.70	LMC 33-4	15.00	0.73	10.36	2.19	0.98	13.67

TABLE 3. (continued)

Star	I_0	$(R\text{-}I)_0$	K_0	$(J\text{-}K)_0$	$(H\text{-}K)_0$	m_{bol}
LMC 33-5	14.39	1.14	10.94	1.69	0.61	14.12
LMC 33-6	13.71	0.96	11.00	1.92	0.78	14.26
LMC 33-7	13.61	1.17	10.63	1.47	0.51	13.69
LMC 33-8	14.55	0.98	11.06	1.34	0.44	14.02
LMC 33-9	13.40	1.14	10.42	1.67	0.63	13.59
LMC 33-10	—	—	9.75	1.73	0.65	12.95
LMC 33-11	14.90	1.14	11.41	1.33	0.46	14.36
LMC 33-12	14.43	1.85	10.43	1.73	0.67	13.63
LMC 33-13	14.17	1.07	10.82	1.75	0.64	14.03
LMC 33-14	14.11	0.78	11.75	1.10	0.30	14.48
LMC 33-15	13.52	0.97	10.60	1.37	0.42	13.58
LMC 33-16	13.82	1.26	10.60	1.58	0.61	13.72
LMC 33-17	13.86	1.08	10.76	1.52	0.51	13.85
LMC 33-18	13.66	0.91	10.95	1.24	0.36	13.82
LMC 33-19	14.03	0.79	11.72	0.97	0.22	14.31
LMC 33-20	13.68	1.20	10.40	1.63	0.62	13.55
LMC 33-21	13.41	1.20	10.08	1.58	0.58	13.20
LMC 33-22	13.66	1.17	10.51	1.57	0.54	13.63
LMC 33-23	14.41	1.60	10.66	1.65	0.65	13.82
LMC 33-24	13.45	1.19	10.20	1.58	0.57	13.32
LMC 37-1	14.12	1.12	10.63	1.46	0.46	13.68
LMC 37-2	13.58	1.24	9.96	1.66	0.61	13.13
LMC 37-3	14.02	0.88	10.90	1.22	0.28	13.75
LMC 37-4	14.11	1.26	10.76	1.65	0.59	13.92
LMC 37-5	15.17	1.30	10.83	2.23	0.93	14.14
LMC 37-6	14.40	1.47	10.77	1.60	0.55	13.90
LMC 37-7	13.63	1.08	10.40	1.41	0.45	13.41
LMC 37-8	14.63	1.01	11.58	1.25	0.34	14.46
LMC 37-9	13.70	0.92	10.86	1.34	0.41	13.82
LMC 37-10	14.35	1.28	10.78	2.02	0.78	14.06
LMC 37-11	14.77	1.09	11.39	1.42	0.43	14.41
LMC 37-12	14.34	0.90	11.25	1.29	0.37	14.17
LMC 37-13	13.99	1.21	10.59	1.64	0.57	13.75
LMC 37-14	13.99	1.22	10.60	1.46	0.48	13.65
LMC 37-16	14.40	1.14	10.64	1.70	0.61	13.82
LMC 37-17	14.32	0.86	11.52	1.22	0.35	14.37
LMC 37-18	14.32	0.91	11.35	1.24	0.31	14.22
LMC 37-19	14.36	1.01	10.77	1.64	0.56	13.93
LMC 37-20	14.45	1.22	10.86	1.70	0.61	14.04
LMC 37-21	13.77	1.27	10.02	1.63	0.59	13.17
LMC 37-22	14.21	1.06	11.26	1.33	0.42	14.21
LMC 37-23	14.02	0.88	10.98	1.18	0.28	13.80
LMC 37-24	—	—	10.71	1.67	0.57	13.88
LMC 37-25	15.28	0.73	13.33	0.91	0.13	15.84
LMC 37-26	13.89	1.12	10.47	1.59	0.56	13.60
LMC 38-1	14.51	1.29	10.80	1.60	0.53	13.93
LMC 38-2	13.76	1.07	10.56	1.39	0.48	13.56
LMC 38-3	14.06	1.45	10.30	1.79	0.67	13.52
LMC 38-4	13.62	0.84	10.76	1.34	0.42	13.72
LMC 38-5	12.85	0.90	9.68	1.30	0.37	12.61
LMC 38-6	14.48	1.21	11.31	1.31	0.42	14.24
LMC 38-7	13.93	1.15	10.22	1.88	0.76	13.47
LMC 38-8	14.11	1.14	10.70	1.61	0.56	13.84
LMC 38-9	14.45	1.13	10.96	1.70	0.67	14.14
LMC 38-10	13.42	1.29	9.51	1.58	0.59	12.63
LMC 38-11	14.28	1.04	10.80	1.06	0.31	13.49
LMC 38-12	14.32	0.91	11.30	1.20	0.31	14.13
LMC 38-13	14.13	1.13	11.01	2.50	1.15	14.31
LMC 38-14	14.28	0.94	11.46	1.13	0.31	14.22
LMC 38-15	14.15	1.02	11.25	1.44	0.47	14.28
LMC 38-16	13.51	0.97	10.21	1.21	0.34	13.05
LMC 38-17	13.59	0.93	10.88	1.16	0.30	13.68
LMC 38-18	13.96	0.98	10.89	1.41	0.42	13.90
LMC 38-19	13.57	1.06	10.39	1.50	0.51	13.47
LMC 38-20	14.38	1.20	10.71	1.79	0.73	13.93
LMC 38-21	13.82	1.35	10.30	1.68	0.63	13.48
LMC 38-22	14.33	0.98	11.55	1.23	0.33	14.41

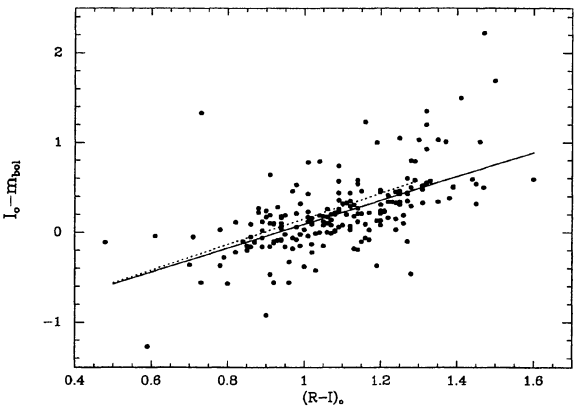

FIG. 1. (I_0-m_{bol}) is shown as a function of $(R-I)_0$ for the 197 LMC field C stars with *RI* and *JHK* photometry (Table 3). The least-squares fit to the data [Eq. (2)] is the solid line. The analogous mean relation obtained by CFPE for SMC field C stars is the dotted line.

3. COLOR–MAGNITUDE AND COLOR–COLOR DIAGRAMS AND THE LUMINOSITY FUNCTIONS

3.1 The Near-Infrared Color–Magnitude Diagram

The m_{bol} vs $(J-K)_0$ diagram for the 204 LMC field C stars with *JHK* photometry given in Table 3 is plotted in Fig. 2. The C stars identified in and around LMC and SMC clusters by FMB are also shown. m_{bol} for the SMC stars was adjusted by −0.3 mag, the assumed difference in distance modulus between the LMC and SMC. As shown by FMB (see their Fig. 4), observed properties of cluster C stars follow well defined trends that are related to the cluster's SWB (Searle *et al.* 1980) type, hence to its age and metallicity. We will interpret our results within the framework setup by FMB for cluster C stars and by Frogel & Blanco (1990) for stars in the LMC Bar West field.

In a near-infrared CM diagram, the region occupied by the SWB III/IV–VI cluster C stars is completely overlapped by our newly observed field C stars. To illustrate this point we have drawn two lines on Fig. 2: the dotted line to the left corresponds to the solid line drawn in Fig. 4 of FMB; this is the dividing line between stars from SWB I–III clusters and stars from clusters of all other types; the dashed line to the right shows the redward limit of cluster C stars. Thus we conclude that our sample of field C stars consists of a composite population with a range of age and metallicity that spans at least the range covered by SWB cluster types III/IV to VI in both Clouds. Based on Fig. 4 of FMB a contribution to the field C star population from stars with ages and metallicities similar to those of SWB III clusters is unlikely but cannot be completely ruled out. As FMB demonstrate, save for one possible case, AGB stars in the youngest clusters (SWB I–III) are all M type, most of which are bluer than the bluest C stars found in the clusters. In addition FMB and Frogel & Blanco (1990) show that the most luminous AGB stars in the clusters and in the Bar West field are M stars from SWB I–III clusters.

The cluster data also suggest that no C stars should appear in the region to the left, i.e., to the blue, of the dotted line in

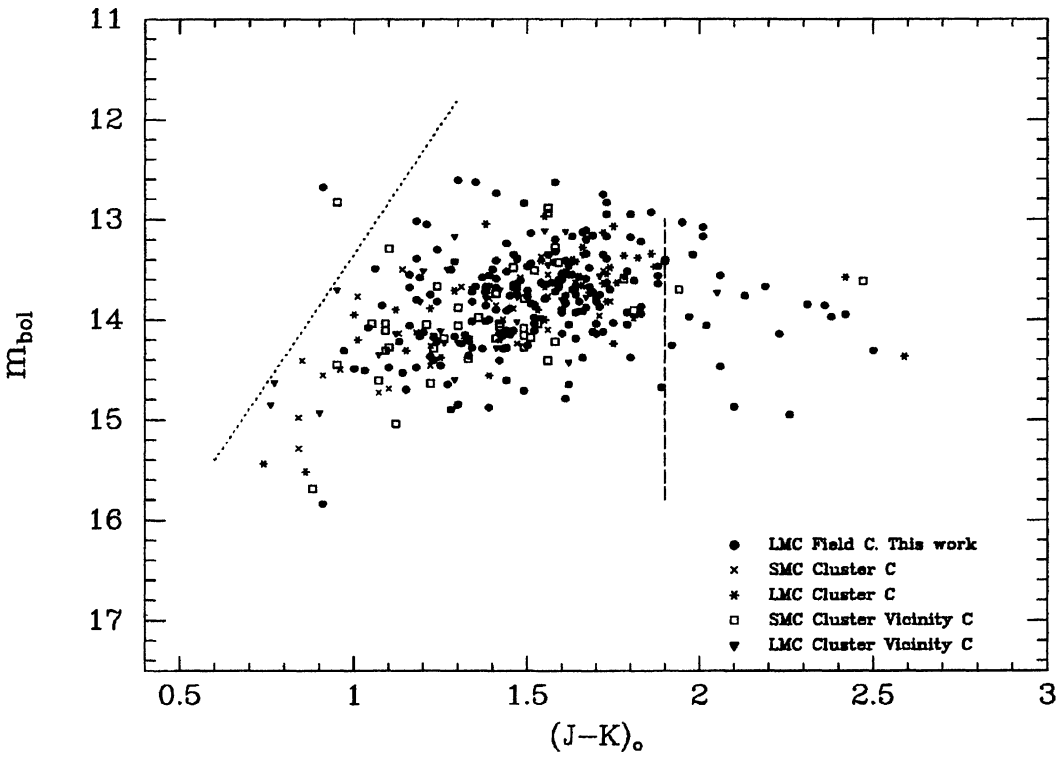

FIG. 2. The filled circles represent the 204 LMC field C stars with *JHK* photometry from Table 2(a). One star is too red to have been plotted on the figure. C stars identified in clusters of the Magellanic Clouds and their vicinity by FMB are also shown. The SMC stars have been brightened by 0.3 mag to compensate for its greater distance modulus. The two straight lines segments delineate the cluster C star region as explained in the text.

Fig. 2; however, two field objects are seen: BMB 12−19 of the LMC and NGC 231-1 of the SMC (classified as a non-member C near the cluster NGC 231 by FMB). Both objects are probable examples of the bluer and hotter group of C stars discovered by Sanduleak & Philip (1977) and further surveyed by Westerlund *et al.* (1986). These stars are generally undetected by surveys of C stars based on identification of the near-IR CN bands as discussed by BM and BMB. The effects of severe crowding in the clusters may further add to the difficulty of detecting the bluest (i.e., weakest CN bands) C stars in them relative to field surveys. A sample of blue C stars—suspected to be CH stars—discovered by Hartwick & Cowley (1988) has been studied recently in the near-IR by Feast & Whitelock (1992) and by Sutzeff *et al.* (1993, hereafter SPE). A straightforward comparison of these two data sets with the present observations (see Secs. 3.2, 3.5) confirms that the former are brighter and bluer as a group than the cool *N*-type carbon stars in the present survey and that of FMB. Nonetheless, we do not think that there is any physical significance to the existence of two groups of C stars. The division merely results from the quite different survey techniques and the biases of each.

C stars such as those found in old, metal-poor, SWB VII clusters are rare in the LMC field sample just as type VII clusters themselves are rare in the LMC. FMB showed that such C stars are almost all fainter and bluer than C stars from any other type of cluster. The few such stars known stand out clearly in Fig. 2 at $m_{bol}>15$. We have found only one field LMC C star (BMB 37−25) with a color and luminosity similar to these SWB VII cluster C stars. The only other field C star seen in this region of Fig. 2 is from FMB; it is found in the vicinity of the cluster NGC 339. Although it may just be a coincidence, we note that NGC 339 is a type VII cluster, so that this star may be a cluster member.

The greatest difference between the field and cluster LMC C star samples that is immediately apparent from inspection of Fig. 2 is the presence of a significant number (23, or 11% of the sample with *JHK* data) of very red ($(J-K)_0$ >1.9) LMC field stars with m_{bol} between 13 and 15. Two other stars in Table 3 have $(J-K)_0$ colors in excess of 3.0, too red for the limits of Fig. 2. Of the 72 C stars identified as Magellanic Cloud cluster members by FMB, only 2 (or 3%) have colors this red. One of these, 1978 IR1, was invisible on the grism survey plates but was discovered while scanning at *K*. Thus it seems that very red C stars are considerably more common in the field population of the Clouds than in the clusters. As pointed out by FMB (see also CFPE) many of these objects may be long-period variables. Cool temperatures and circumstellar dust shells could account for their red colors. Furthermore, their red colors probably result in an underestimation of their bolometric luminosities since the observations extend only to the *K* band. That this could be the case is suggested by the red *K-L* colors that some of the reddest cluster C stars were found to have (Table 2 of FMB). $(R-I)_0$ colors are available for 20 of the 23 field C stars with $(J-K)_0 \geq 1.9$. They are not distinctive but lie in the range $0.8<(R-I)_0<1.5$ comparable to the other C stars observed.

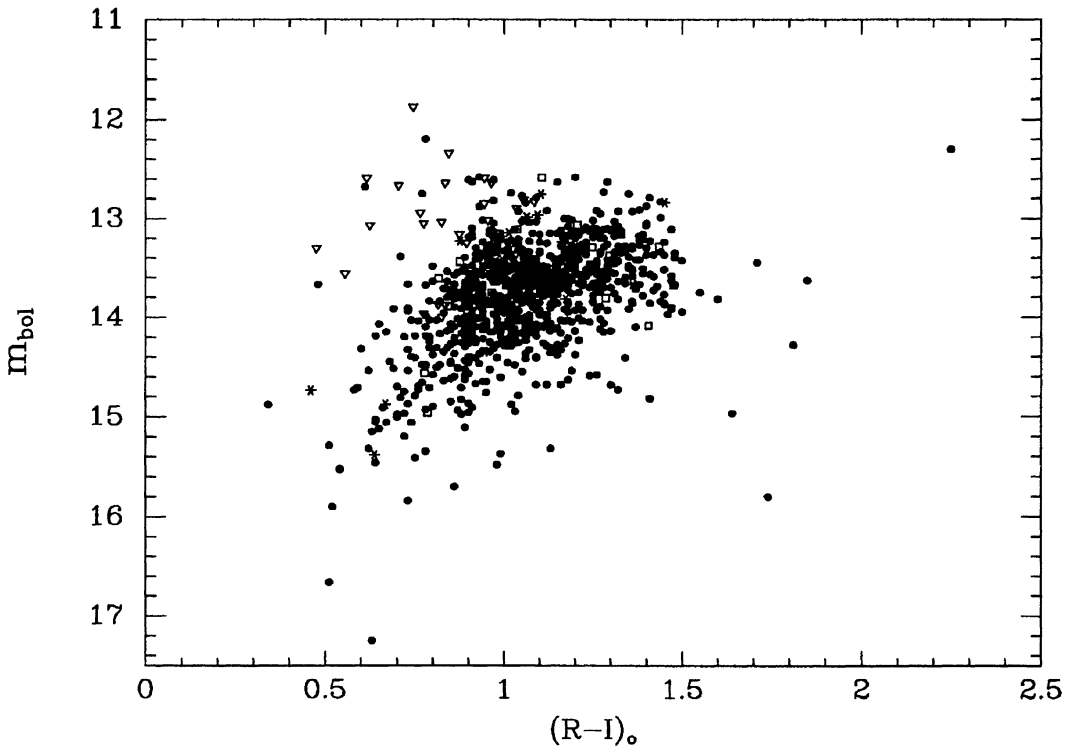

FIG. 3. The m_{bol} vs $(R-I)_0$ color–magnitude diagram for the 923 LMC field C stars with *RI* photometry given in Table 2. The 888 stars from the surveys of BMB and BM are shown as filled circles; the 35 stars from the survey of WORC are shown as open squares. For comparison, we have included in the figure the 39 blue C stars from the list of Hartwick & Cowley (1988) with *RI* photometry by SPE (open triangles); and 19 C stars from the sample of BMB observed by Richer (1981) in the LMC "Bar-West" field (asterisks).

FMB suggested that the Bar West field has a somewhat greater percentage of metal-rich stars than their cluster sample based on the presence of an excess of red, luminous M stars in the field. Higher metallicity might be expected to produce redder C stars since the evolutionary track of such a star will be shifted to cooler temperatures than that of a lower metallicity star of the same luminosity. Aside from this effect, the formation of molecules and grains should be enhanced in the higher metallicity star due to both lower temperatures and larger numbers of heavy atoms. These enhancements could, in turn result in increased blanketing by molecular absorption bands, higher mass loss rates (cf. Groenewegen *et al.* 1995), and increased circumstellar thermal emission. We also point out that for the same age a higher metallicity star will have a greater mass than a lower metallicity star, so that evolution on the AGB would terminate at a brighter magnitude for the former star. Also, the luminosity which marks the transition between M and C stars would be brighter in the more metal-rich population.

Other more subtle differences between the field and the cluster population are also suggested by Fig. 2. Excluding C stars from SWB type VII clusters, which as mentioned above are significantly less luminous as a group than any other C stars, it seems that the LMC field C sample has a slightly fainter low luminosity limit (about 0.2 mag fainter, at $m_{bol}\sim15$) than the cluster sample. At the same time, the bright luminosity limit of the field sample seems to be about 0.4 mag brighter (at $m_{bol}\sim12.6$) than that of the cluster population, although this latter difference depends on only a few stars. Although these differences can also be seen in an m_{bol} vs $(R-I)_0$ plot and in the luminosity functions (see discussion in next two sections), they are not statistically significant.

3.2 The m_{bol} vs $(R-I)_0$ Diagram

The m_{bol} vs $(R-I)_0$ diagram for 923 stars with *RI* photometry in Table 2 is shown in Fig. 3 (for the subset with *JHK* observations, m_{bol} values are from Table 3). These stars include the 888 field LMC C stars from BMB and BM, and the 35 LMC field C stars from WORC. For comparison purposes we have included in the figure 39 blue C stars (the open triangles) from the list of Hartwick & Cowley (1988) with *RI* (kc) photometry by SPE. These latter data were corrected for reddening with the reddening law as in Sec. *2.4* and $E(B-V)=0.12$ from SPE. The bolometric magnitudes, not published by SPE, were obtained from Suntzeff (private communication). Figure 3 shows that these stars form a group bluer and brighter in the mean, with $\langle(R-I)_0\rangle=0.89$ and $\langle m_{bol}\rangle=13.21$, than the *N*-type C stars observed by us for which $\langle(R-I)_0\rangle=1.08$ and $\langle m_{bol}\rangle=13.80$. Also included in Fig. 3 are 19 C stars of the LMC Bar West field observed by Richer (1981) but not by us. His *RI* photometry in the Johnson system was de-reddened and transformed to the Kron–Cousins system using procedures detailed in Sec. 4. m_{bol} was then obtained using Eq. (2). Not surprisingly, these stars occupy the same region of the CM diagram in Fig. 3 as our C stars.

With a significantly bigger sample of stars, the m_{bol} vs

$\langle (R\text{-}I)_0 \rangle$ diagram is consistent with its near-IR counterpart (Fig. 2) in suggesting that the range in luminosity of the LMC field C stars is larger than that of the cluster population (but see the discussion in the next section below). With the exception of two objects, BMB BW-74 and BMB 16−39, the upper luminosity limit of the field population is well defined in Fig. 3, at about $m_{bol}=12.6$, 0.4 mag brighter than that of the cluster population. Figure 3 also shows that the low luminosity limit of the field sample appears to be lower than that of the cluster sample. One must keep in mind, though, that Eq. (2), used to estimate the m_{bol} values for the stars without *JHK* photometry, will introduce additional scatter into Fig. 3. Also, since the stars that are faintest in m_{bol} in Fig. 3 will also tend to be among the faintest in *I*, effects due to misidentification (some could be M stars) and crowding could become important.

A straightforward interpretation of possible differences in luminosity limits between the cluster and field sample of C stars would be that the composite population of field LMC C stars has a more extreme range of age and metallicity than the cluster C sample. In agreement with current carbon star formation theories (see, e.g., Iben & Renzini 1983), which predict that older age and/or lower metal abundance results in the formation of C stars at a lower luminosity, the presence of a somewhat older and/or more metal poor component of C stars in the field, not present in the clusters, would explain the existence of the fainter field C stars seen in Figs. 2 and 3. The presence of the component of brighter stars in the field is explained, on the other hand, by exactly the opposite effect: younger age and/or higher metallicity. We have already advanced the possibility of higher metallicity for the field stars to explain their greater percentage of extremely red stars. However, it should be kept in mind that the sample of clusters studied by FMB may not be representative of the whole system of clusters of the Magellanic Clouds.

Finally, we point out there are only two C stars in our sample of about 900 more luminous than $m_{bol}=12.5$, [$M_{bol}=-6.0$ for $(m-M)=18.5$], thus confirming the well-know disagreement, discussed extensively by FMB and SPE, between observations and early theoretical models, which predicted the existence of AGB stars as bright as $M_{bol}=-7.2$ (e.g., Iben & Renzini 1983).

3.3 The Luminosity Functions

The first complete Magellanic Cloud C star luminosity function based on the *I* magnitudes from BMB's survey and revised with CFPE's *JHK* photometry differed grossly from theoretical predictions (see, for example, CFPE; Iben 1981; Iben & Renzini 1983; Renzini & Voli 1981). The results of surveys for C stars in the LMC over an area more than an order of magnitude larger than the BMB survey (Westerlund *et al.* 1978; Richer 1981) did not reduce the discrepencies between theory and observation. Subsequently, intensive work on revisions and additions to the theory of stellar evolution along the AGB and of C star formation resulted in what now appears to be reasonable agreement with empirical luminosity functions and other empirically derived C star parameters (see, for example, reviews by Iben 1988; Lattanzio 1989b; and Groenewegen & de Jong 1993). This section

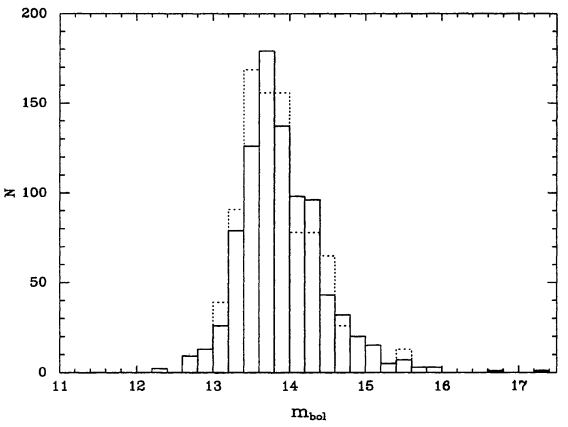

FIG. 4. The solid line is the apparent bolometric luminosity function for the 895 Blanco LMC field C stars from Tables 2(a) and 3. The dashed line is the apparent bolometric luminosity function for the 69 C stars identified in SWB 3.5−6.5 clusters of the Magellanic Clouds by FMB scaled by the ratio of the numbers, that is, 895/69.

examines the luminosity function for the C stars in our sample and compares it with the function for cluster C stars (FMB[5]).

The bolometric luminosity function for the 895 Blanco LMC field C stars from Tables 2(a) and 3 is plotted in Fig. 4 and enumerated in Table 4. In Fig. 4 we also show this function (dashed line) for C stars in SWB 3.5−6.5 clusters of the Magellanic Clouds (FMB) scaled by the ratio between the number of field and cluster C stars in the samples, namely, 895/69. Table 5 lists the mean values, dispersions, and peak values of the various luminosity functions. To facilitate comparisons, all luminosity functions considered were constructed with the same bin centers. m_{bol} for the SMC stars has been brightened by 0.3 mag.

While comparison of the two luminosity functions in Fig. 4 suggests the presence of faint and bright tails to the field star luminosity function relative to that for the cluster stars as noted in Secs. *3.1* and *3.2*, inspection of this figure shows that these differences can be made to vanish with the addition of only a few stars to the faint and bright ends of the cluster function. In fact, Student *t* and *F* tests on the luminosity functions listed in Table 5 reveal only one significant (at the 95% level) difference—consistent with the findings of FMB based a small sample of LMC field stars—namely, between the SMC and the LMC. This difference, of course, is sensitive to the adopted relative distance modulus of the two Clouds. The fact that the *F* test for differences in the variances shows no significant difference between the LMC cluster and field samples implies that the tails to the latter function that we have noted are most likely due to small number statistics (we do note, though, that the SMC SWB 3.5−6.5 cluster C star and the SMC cluster vicinity C star

[5]Note, though, that three cluster C stars listed by FMB will be excluded from the comparison (although this in no way changes the results): the two C stars from the SWB type VII clusters in the SMC (stars this blue and faint would probably have been missed by the grism survey) and one LMC star classified as CM. Thus the LFs we present based on the FMB data will be closely similar but not identical to those given by FMB.

TABLE 4. The apparent bolometric luminosity function for LMC field C stars.

Bin Center (m_{bol})	# of C Stars	% of Total
12.1	0	0.0
12.3	2	0.2
12.5	0	0.0
12.7	9	1.0
12.9	13	1.4
13.1	26	2.9
13.3	79	8.8
13.5	126	14.1
13.7	179	20.0
13.9	137	15.3
14.1	98	11.0
14.3	96	10.7
14.5	43	4.8
14.7	32	3.6
14.9	20	2.2
15.1	15	1.7
15.3	5	0.6
15.5	7	0.8
15.7	3	0.3
15.9	3	0.3
16.1	0	0.0
16.3	0	0.0
16.5	0	0.0
16.7	1	0.1
16.9	0	0.0
17.1	0	0.0
17.3	1	0.1
17.5	0	0.0

luminosity functions show a similar difference in that there are a couple of stars in the field sample brighter and fainter than the brightest and faintest cluster stars). Therefore, we conclude that the one significant difference between cluster and field C stars is the presence of a population of red stars in the field sample not present in the cluster sample.

3.4 The Near-Infrared Color–Color Diagram

The near-infrared two-color diagram for the LMC field C stars from Table 3 is plotted in Fig. 5 (one of the stars from Table 3 falls off the limits of the figure). In agreement with previous results (e.g., CFPE), Fig. 5 shows that the $(H-K)_0$ and $(J-H)_0$ colors are highly correlated. A least-squares fit to the data gives

$$(J-H)_0=0.62(H-K)_0+0.67. \quad (3)$$

This mean relation is shown as a solid line in Fig. 5. For comparison purposes we have included in Fig. 5 the C stars identified in clusters of the Magellanic Clouds and their vicinity by FMB, and 20 C stars identified by BMB in the SMC, with *JHK* photometry by CFPE. Also for comparison, we have drawn in Fig. 5 the mean relations for galactic C stars (dotted straight line) and galactic field M stars (dot-dashed curved line) from CFPE and Frogel *et al.* (1978), respectively. In agreement with CFPE (see also Fig. 9 in Westerlund *et al.* 1991), Fig. 6 shows systematic differences between the colors of C stars from the LMC, the SMC, and the Galaxy. Since the trend in the differences is in the same order as mean metallicity differences between the three galaxies, CFPE suggested that it arises from a metallicity-related blanketing effect.

Figure 5 demonstrates that the redness of the LMC field C stars compared to the cluster C stars seen on the near-infrared CM diagram (Sec. *3.1*) is clearly visible in the $(H-K)_0$ vs $(J-H)_0$ plane as well (only two LMC cluster C stars are seen redder than $(H-K)_0\sim0.75$). Finally, we point out that although it appears from Fig. 5 that the galactic C stars from CFPE do not span as extreme a color range as our LMC field C stars, the galactic sample is too small to make a meaningful comparison.

3.5 The $(J-K)_0$ vs $(R-I)_0$ Diagram

The $(J-K)_0$ vs $(R-I)_0$ two-color diagram for the 197 LMC field C stars with both *RI* and *JHK* photometry (Table 3) is plotted in Fig. 6. With the exception of high $(J-K)_0$, low $(R-I)_0$ combinations, the $(J-K)_0$ and $(R-I)_0$ colors of the LMC field C stars are well correlated, although not as tightly as their near-infrared colors. Excluding 14 outliers, most of which are those stars already noted as having exceptionally red $J-K$ colors, a least-squares fit to the data gives

$$(R-I)_0=0.51(J-K)_0+0.31. \quad (4)$$

This mean relation is shown as a solid line in Fig. 6. The fact that the reddest in $(J-K)$ C stars are not particularly red in $(R-I)$ suggests that molecular blanketing effects are particularly enhanced for these stars. We note, though, that on an m_{bol}, $(R-I)_0$ plot (Fig. 3) these stars are not distinguishable. In Fig. 1 these stars tend to lie in the upper right.

We have also plotted in the figure 20 blue C stars from the list of Hartwick & Cowley (1988), with RI_{kc} and *JHK* photometry by SPE. SPE's results were de-reddened as explained in Sec. *3.2*. Inspection of Fig. 6 shows that although

TABLE 5. Carbon star bolometric luminosity functions.

Sample	#Cs	Mean m_{bol}	σ	Peak m_{bol}
This work - all stars. (Fig. 4)	895	13.80	0.55	13.70
This work - stars w/ RI & JHK photometry	197	13.80	0.50	13.70
FMB - LMC cluster vicinity	39	13.88	0.44	13.70
FMB - SMC cluster vicinity	45	13.99	0.54	14.10
FMB - LMC+SMC cluster vicinity	84	13.94	0.49	13.7/14.1
FMB - LMC SWB 3.5-6.5 cluster members	43	13.78	0.54	13.50
FMB - SMC SWB 3.5-6.5 cluster members	26	14.00	0.39	13.7/13.9
FMB - LMC, SMC SWB 3.5-6.5 cluster members. (Fig. 5)	69	13.86	0.50	13.50

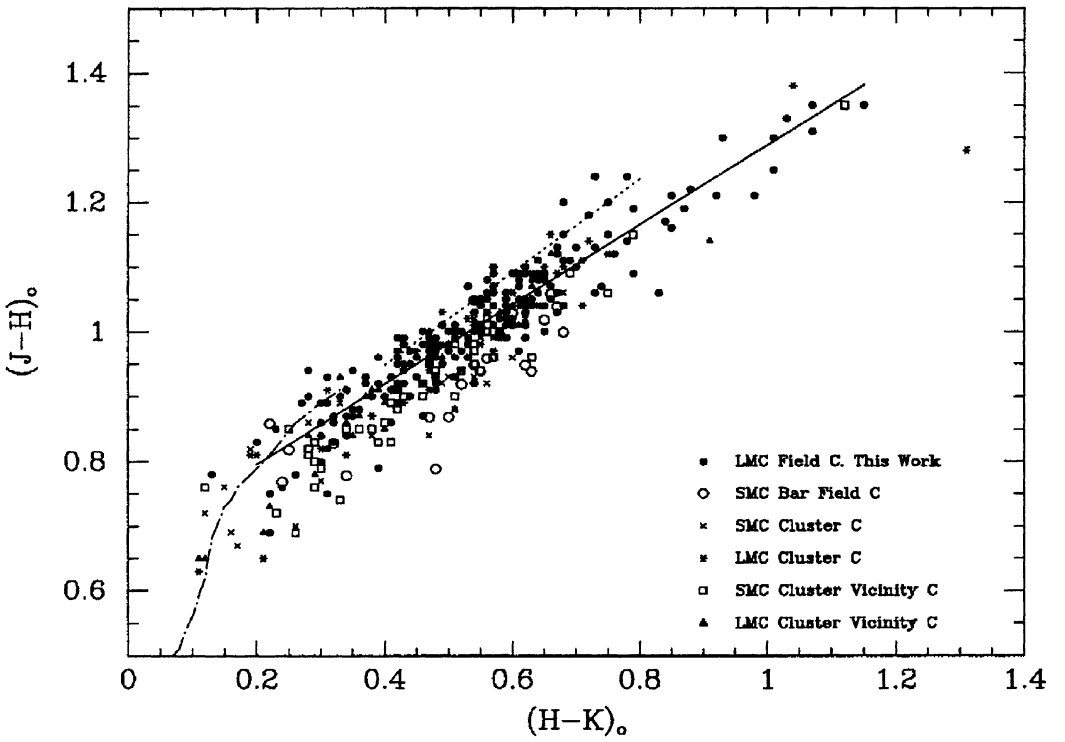

FIG. 5. The near-infrared color–color diagram for the 204 LMC field C stars with *JHK* photometry given in Table 3 (filled circles). The C stars identified in clusters of the Magellanic Clouds and their vicinity by FMB are also shown. The symbol code for them is the same as in Fig. 2. We have also included in the figure 20 C stars identified by BMB in the "Bar" field of the SMC with *JHK* photometry by CFPE (open circles). The least-squares fit to the data [Eq. (3)] is plotted as a solid line. For comparison, we have drawn in the figure the mean relations for galactic C stars (dotted straight line) and galactic field M stars (dot-dashed curved line), from CFPE and Frogel *et al.* (1978), respectively.

these latter stars extend to bluer colors, they merge smoothly with the bluest stars of our sample. This is a good illustration of the probable overlap, both in terms of observed and physical properties, between these blue C stars and the *N*-type C stars from our sample. A simple comparison in the near-infrared color–color plane shows a very similar effect. Also shown in Fig. 6 are 20 C stars identified by BMB in the "Bar" field of the SMC, with RI_{kc} photometry by BMB and *JHK* photometry by CFPE. In spite of the dispersion shown by these stars [probably due to only fair-quality photographic $(R-I)$ colors], it is clear from the figure that the SMC field C stars are systematically bluer in $(R-I)_0$, for a given $(J-K)_0$, than the LMC field C stars. This is consistent with the offset observed in the near-infrared color–color diagram (Fig. 5) between the LMC C and SMC C stars, and may also be due to a metallicity-related blanketing effect.

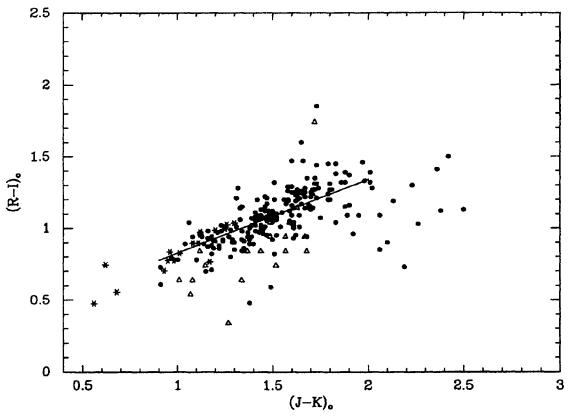

FIG. 6. The $(J-K)_0$ vs $(R-I)_0$ color–color diagram for the 197 LMC field C stars with both *RI* and *JHK* photometry given in Table 3. The least-squares fit to these data [Eq. (4)] is plotted as a solid line. For comparison, we have included in the figure the 20 C stars identified by BMB in the "Bar" field of the SMC, with *RI* photometry by BMB and *JHK* photometry by CFPE (open triangles); and 20 blue C stars from the list of Hartwick & Cowley (1988), with *RI* and *JHK* photometry by SPE (asterisks).

4. THE THEORETICAL HR DIAGRAM

The M_{bol} vs log T diagram for all the LMC C stars in the present study is shown in Fig. 7. $(m-M)_0=18.5$ was adopted as the distance modulus of the LMC. Since most temperature–color relations for C stars are given for colors on the Johnson (1964) system, we had to transform our $(R-I)$ and $(J-K)$ colors to the Johnson system. To accomplish this, a series of intermediate steps was necessary as described below. Then we will discuss the physical significance of color temperatures for C stars.

4.1 Transformation of the RI Kron–Cousins (kc) Photometry to the Johnson (j) System

Forty-six C stars of the LMC Bar-West field observed by us in the *RI* (kc) system have also been observed by Richer

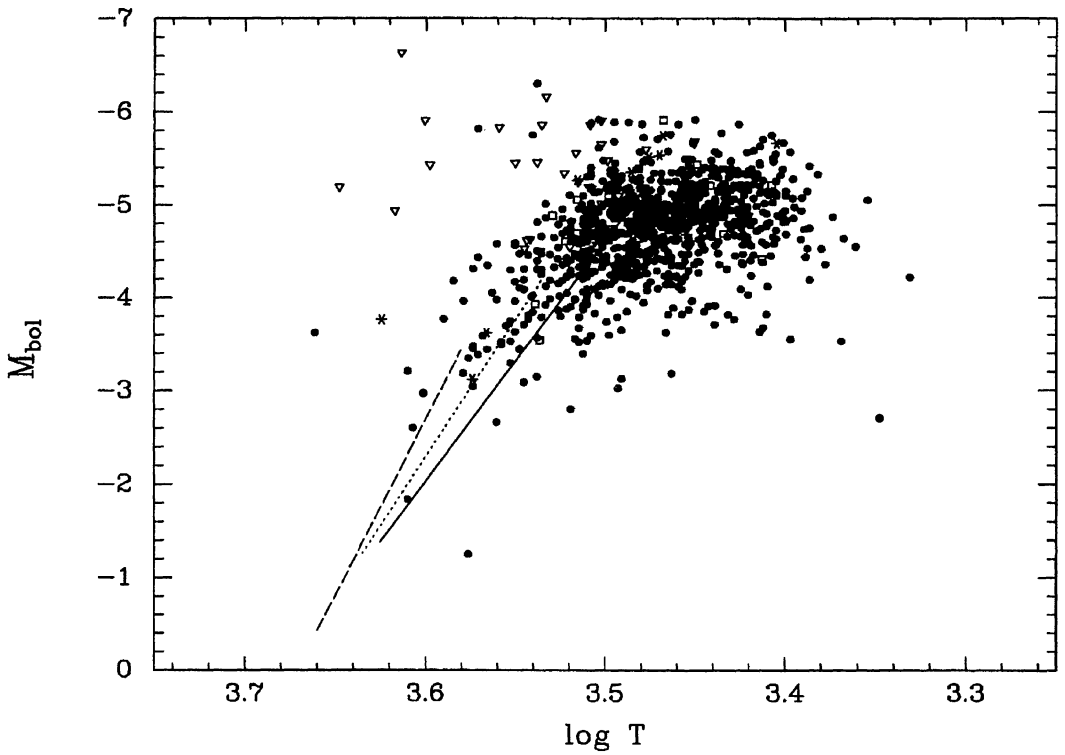

FIG. 7. The theoretical HR diagram for the 930 LMC field C stars from Tables 2 and 3. The 895 stars from the surveys of BMB and BM are shown as filled circles; the 35 stars from the survey of WORC are shown as open squares. Other objects included for comparison have the same symbol code as in Fig. 3. The lines plotted correspond to AGB evolutionary tracks from core helium exhaustion to the first major thermal pulse from models with $\alpha=1.0$ by Lattanzio (1986,1991). The dashed line is for a 1.0 $\mathcal{M}_\odot$ Pop II star with $(Y,Z)=(0.2,0.001)$, the dotted line to a 2.5 $\mathcal{M}_\odot$ Pop I star with $(Y,Z)=(0.3,0.01)$, and the solid line to a 4.0 $\mathcal{M}_\odot$ Pop I star with $(Y,Z)=(0.2,0.02)$. See text for details.

(1981) in the Johnson system. To compare our results with those of Richer, Richer's photometry was first corrected for reddening by means of the reddening law derived by CFPE for the Johnson RI system, using the same $E(B-V)$ value (0.17) we adopted for that field. A least-squares fit to the data in common, using our $(R-I)_{0,kc}$ values as independent parameter, yielded the following:

$$(R-I)_{0,j}=1.01(R-I)_{0,kc}+0.12. \quad (5)$$

Equation (5) was applied to all our stars with RI(kc) photometry to obtain their $(R-I)_0$ colors in the Johnson system.

4.2 *Transformation of the $(J-K)_{cit}$ Colors to the Johnson System*

Jones & Hyland (1980) have demonstrated that $(J-K)_j=(J-K)_{AAO}$ while Elias *et al.* (1983) have shown that $(J-K)_{cit}=0.897(J-K)_{AAO}+0.006$. Thus we arrive at the following equation to transform our $(J-K)_0$ colors (on the CIT/CTIO system) to the Johnson system:

$$(J-K)_j=1.115(J-K)_{cit}-0.007. \quad (6)$$

4.3 *Temperatures*

Ridgway *et al.* (1980b) demonstrated that color temperatures of C stars as derived from broadband photometry are not directly related to their effective temperatures as derived from direct determination of their radius and luminosity. The extremely red colors of C stars are not due to low temperatures but arise primarily from molecular line blanketing from carbon species. The net result of this is an underestimation of T_{eff} when it is determined from color data alone. Keeping in mind that the relationship between color temperature and effective temperature for C stars is uncertain, it nonetheless proves to be instructive to estimate temperatures for the C stars from the $(J-K)_j$ and/or $(R-I)_j$ colors given here. These temperatures combined with bolometric magnitudes derived earlier then permit us to make a comparison with predicted evolutionary tracks for C stars. Correlations between color and effective temperature for C stars, based on various sets of assumptions, have been discussed, for example, by Mendoza & Johnson (1965, hereafter MJ), Scalo (1976), and Bessell *et al.* (1983, hereafter BWE).

4.3.1 *Temperatures from the $(R-I)_j$ colors*

Under the assumption that C stars radiate like ordinary K and M giants, Mendoza & Johnson (1965), using the procedure of Johnson (1964), tabulated relations between T_{eff} vs $(R-I)_j$ and T_{eff} vs $(J-K)_j$ for them. From Tables 1 and 2 of MJ, we have determined the following correlation:

$$T1=6603-5498(R-I)_j+2743(R-I)_j^2-563(R-I)_j^3 \quad (7)$$

with $0.5<(R-I)_j<1.8$. This relation is similar to one given by Wallerstein (1973). Equation (7) was applied to all stars

in our sample to obtain a first estimate for $T_{\rm eff}$ called $T1$. Note that for the group of C stars with particularly red $J-K$ colors temperature estimates from their $(R-I)$ colors may be strongly affected by blanketing (Sec. *3.5*).

4.3.2 Temperatures from the $(J-K)_j$ colors

In a similar manner, we have derived the following from Tables 1 and 2 of MJ:

$$T2=6194-3264(J-K)_j+692(J-K)_j^2 \quad (8)$$

with $0.5<(J-K)_j<2.3$. This equation was applied to the 204 C stars from our sample with $(J-K)_j$ colors to obtain a second estimation of $T_{\rm eff}$, $T2$.

A third, independent, estimation of $T_{\rm eff}$ from the $(J-K)_j$ color was obtained for the above sample by means of the relation given by BWE:

$$T3=7070/[(J-K)_j+0.88] \quad (9)$$

with $0.5<(J-K)_j<2.0$. This relation was established by BWE from JHK photometry and $T_{\rm eff}$ derived from occultation angular diameters for C and M stars by Ridgway *et al.* (1980a and 1980b, respectively). As shown by Fig. 4 of BWE, M giants and C stars appear to form a continuous sequence in the $\log T_{\rm eff}-(J-K)_j$ plane which is well fit by Eq. (9).

For the 197 C stars of our study with both RI and JHK photometry, we took an average of the three estimates of $T_{\rm eff}$, $T1$, $T2$, and $T3$. For the stars with only RI data, $T1$ was used as a measure of $T_{\rm eff}$. A temperature was calculated for every star regardless of the limits imposed by Eqs. (7), (8), and (9). Analysis of the individual $T1$, $T2$, and $T3$ values obtained for the stars with both RI and JHK data shows that the three methods give fairly consistent results, provided that both $(J-K)_j<1.9$ and $(R-I)_j>1.0$ were satisfied. For this group of objects the overall averages are: $\langle T1\rangle=T(R-I)_{mj}=2903\pm205$ K, $\langle T2\rangle=T(J-K)_{mj}=2797\pm191$ K and $\langle T3\rangle=T(J-K)_{\rm bwe}=3035\pm173$ K. For each star, we obtained $\langle T\rangle$, sigma; the mean standard deviation is: $\langle$sigma$\rangle=138$ K. For colors outside the above ranges, the agreement is maintained to a lesser degree, except for cases of very low $(R-I)_j$ and/or very high $(J-K)_j$. For these latter, the temperatures from the $(J-K)_j$ color remain fairly consistent, but $T1=T(R-I)_{mj}$ is clearly higher. For the few cases with $(J-K)_j$ in excess of 3.0, everything breaks down probably because of extreme blanketing and a possible contribution from thermal emission or from circumstellar reddening.

4.4 Comparison with Theoretical Results

A comparison of the distribution of the LMC field C stars in the $M_{\rm bol}$, $\log T$ plane with selected evolutionary models permits a test of some theoretical predictions. Figure 7 shows evolutionary tracks from the early AGB, corresponding to core helium exhaustion, to the first major thermal pulse (defined as the first pulse of sufficient strength to drive the intershell convective zone just outside the helium burning shell) according to models with α (ratio of mixing length to pressure scale scale height)=1 by Lattanzio (1986, 1991). The dashed line corresponds to a 1.0 $\mathcal{M}_\odot$ star with $(Y,Z)=(0.2,0.001)$. Based on calculations for a 0.8 $\mathcal{M}_\odot$ star with identical composition, Lattanzio (1989a) concluded that 1.0 $\mathcal{M}_\odot$ is about the minimum mass required for dredge-up to occur in a Population II AGB star. Recall that dredge-up is necessary to produce most if not all carbon stars. Since this model neglects mass loss, its true main sequence turnoff mass would have to be higher. The dotted and solid lines in Fig. 7 correspond to Population I models with 2.5 $\mathcal{M}_\odot$, $Y=0.30$, $Z=0.01$ and 4.0 $\mathcal{M}_\odot$, $Y=0.20$, $Z=0.02$, respectively. The quoted masses are also initial main sequence masses with mass loss neglected. These three models qualitatively correspond to the ranges in metallicity and age exhibited by LMC clusters of SWB types III/IV to VI (see Table 3 in FMB), which, as shown here (and by FB for M stars), are also appropriate to the LMC field C stars from our study.

From Fig. 7 we draw one of the main conclusions of this paper: 1 $\mathcal{M}_\odot$ is the smallest stellar mass that will produce a Pop II LMC field C star. This is in agreement with Latanzio's predictions of the minimum mass required for dredge-up to occur and with a similar conclusion drawn by FMB from their observations of cluster stars. Also, the lower bound to the luminosity of the C stars in Fig. 7 corresponds quite well with the luminosity at which the first major thermal pulse of the 1 $\mathcal{M}_\odot$, Pop II model occurs, an event which can be considered to define the transition from M type to C on the AGB. The detection of a small percentage of stars with $\mathcal{M}_{\rm bol}$ fainter than the transition luminosity from M to C type for this model is consistent with this picture: postflash luminosity dips (see, e.g., Iben & Renzini 1983) can place a C star approximately 1/2–1 mag below its transition luminosity, (we cannot rule out the possibility that the position of some of the faintest C stars could be the result of misidentifications and measurement errors).

Keeping in mind the possible existence of uncertainties in the temperatures of our C stars derived from their broadband colors (Sec. *4.3*), Fig. 7 suggests additionally that the 1 $\mathcal{M}_\odot$, Pop II model represents the hot limit for LMC C stars. Furthermore, comparison with Fig. 4 of Westerlund *et al.* (1995) shows that their locus for the onset of the first He flash in a double shell burning star in the LMC (based on the observed transition between M, S, and C stars) lies close to the hot side of the distribution of most of the stars in Fig. 7. Consideration of the $\alpha=1.5$ models does not change this result since, as pointed out by Lattanzio (1991), the only difference in the evolutionary tracks of models that differ only in the value of α are slightly higher temperatures for higher values of α.

Finally, the location of the Pop I models in Fig. 7 with higher mass and Z shows that to form C stars from metal rich, relatively young stars, one must go to higher luminosities and cooler temperatures. These models probably represent the upper bound to the physical properties of the C stars in our field sample.

5. PROPERTIES OF THE LMC CARBON STARS AS A FUNCTION OF POSITION IN THE LMC

There are several easily measurable characteristics of carbon stars that can serve as indicators of the age and chemical abundance of the stellar population of which the C stars are members. Two such characteristics are the ratio of the number of C stars to the number of M stars and the transition luminosity as defined by FMB—the average luminosity of the brightest M stars and the faintest C stars. In this section we will combine the LMC survey data for M and C stars given by BM with the bolometric luminosities calculated here and attempt to map out stellar age and chemical abundance variations across the face of the LMC. Costa (1990)—from *RI* photometry of the C stars identified by BM in four fields of the LMC (LMC 12, 17, 20, and 32)—presented evidence that the mean photometric properties of the LMC C stars changed with position. Based on the ages of the star clusters in which C stars are found (see FMB), the approach we are taking will be effective for stars with ages between a few Gyr and about 100 Myr.

We begin by defining an ad-hoc (X,Y) coordinate system based on the isopleths of carbon star frequencies illustrated in Fig. 3 of BM. The (0,0) of this coordinate system is defined to be BM's field 26 (LMC O, the optical center of the LMC). The X axis is parallel to the major axis of the innermost isopleth while the Y axis is perpendicular to it. Radial distance in the plane of the sky from the center of the LMC is therefore $(X^2+Y^2)^{1/2}$. (X,Y) values are the distances of the field centers in degrees from the origin as measured on BM's Fig. 3. Positive values of X and Y are towards the east and north, respectively. Since the innermost isopleths of C star frequency are well aligned with the Bar of the LMC, the Y coordinate of any field is essentially equivalent to the distance of that field from the Bar. Although somewhat crude, this coordinate system will be seen to serve its purpose rather nicely. Tables 6 and 7 list the quantities that will be needed for the analysis presented in this section.

The first two columns of Table 6 identify the LMC field with the designation given by BM and the number of C stars with *RI* photometry (Table 2); the numbers in parentheses are how many C stars were identified by BM. The next three columns contain the average magnitudes and colors for the stars observed in each field based on the values given in Table 2. Immediately underneath each average value is its one sigma dispersion. Then comes the transition luminosity $[m_{\rm bol}(t)]$ from M to C type as defined below. Since for most stars $m_{\rm bol}$ was determined from *RI* observations alone via Eq. (2), we also present in the last 5 columns of Table 6 similar data as in cols. 2–5 but now only for those stars that have both *RI* and *JHK* photometry. The average $m_{\rm bol}$ values in the last column of Table 6 are those based on *JHK* photometry alone. For those fields with *JHK* photometry, there is no significant difference between the average $m_{\rm bol}$ derived directly from the *JHK* data and that derived indirectly via Eq. (2).

Table 7 gives the (X,Y) values for each field and its distance from the origin, statistics on the number of C and M stars in the fields (from BM), and the NGC number and SWB type of any cluster present in the field as indicated in Fig. 3 of BM. Finally, we note that we have considered only M stars of spectral types equal to or later than M5 since BM state that their statistics are incomplete for earlier type M stars.

5.1 Average Magnitudes and Colors

We searched for spatial trends in the mean values of the reddening and extinction corrected *RI* and *JHK* colors and magnitudes and of $m_{\rm bol}$ for the C stars in each field by testing for dependencies of these quantities on X, Y, and r. No dependences of mean colors or magnitudes on position were found with a significance greater than the one sigma dispersions in the means themselves. We note that typical dispersions in the magnitudes are greater than 0.4 (Table 6). Thus, Costa's (1990) suggestion that there is some spatial dependence of the mean *RI* colors of C stars in the LMC is not supported and must have arisen because of the small number of fields he observed. We of course cannot rule out that small spatial gradients in the colors or magnitudes are masked by the intrinsic dispersion in the quantities themselves.

5.2 The Transition Luminosity

In their study of the AGB of Magellanic Cloud clusters, FMB clearly demonstrated that for clusters that contain both C and M stars there exists a transition luminosity $m_{\rm bol}(t)$ between the faintest C stars and the brightest M stars and that this transition luminosity is correlated with the cluster's SWB type and thus with its age and metallicity in the sense that the luminosity increases with increasing Z and decreasing age. Although the LMC field C stars we have observed must have a significant spread in both age and metallicity, the concept of a transition luminosity may still prove to be useful in searching for differences in these quantities between the areas surveyed. Lacking photometry of the M stars, we attempt to estimate $m_{\rm bol}(t)$ for each field from the luminosity of the C stars alone by taking the average magnitude of the four faintest C stars in a field. These values are listed in Table 6. Other estimates for $m_{\rm bol}(t)$ such as the median magnitude of the 3 or 4 faintest C stars in a field yield values for $m_{\rm bol}(t)$ that are with 0.1 mag of that calculated from the average of the 4 faintest. We only considered those 36 fields all or nearly all of whose C stars were observed, and then only if there were at least 8 C stars in each.

The transition luminosities for the LMC fields given in Table 6 are almost all between $m_{\rm bol}=14.0$ and 15.0. This is comparable to the fainter transition luminosities that are seen in SWB V–VI type Magellanic Cloud clusters observed by FMB (see their Table 3 and Fig. 14) and significantly fainter than the transition luminosities of the earlier, i.e., III–IV, SWB types which are between 13.1 and 13.5. Since the technique used by FMB to calculate transition luminosities involved averaging together $m_{\rm bol}$ of the faintest C stars with $m_{\rm bol}$ of the brightest M stars, and since the brightest M stars are typically fainter than the faintest C stars in any given cluster by a few tenths of a magnitude, the $m_{\rm bol}(t)$ values in Table 6 would need to be made yet fainter for a proper comparison with the FMB values.

TABLE 6. Average magnitudes and colors with their respective sigmas.

	All Stars					Stars with *RI* and *JHK*				
Field	#C stars observed	I_0	$(R\text{-}I)_0$	m_{bol}	$m_{bol}(t)$	#C stars observed	K_0	$(J\text{-}K)_0$	$(H\text{-}K)_0$	m_{bol}
LMC BW	48(70)	13.79	1.12	13.51	14.3	17(70)	10.46	*1.54*	0.54	13.55
		0.48	0.23	0.43			0.49	*0.18*	0.12	0.47
LMC O	13(79)	13.87	1.13	13.70		10(79)	10.54	*1.63*	0.59	13.64
		0.42	0.19	0.49			0.62	*0.35*	0.22	0.53
LMC R	7(37)	13.76	1.28	13.22		7(37)	10.04	*1.71*	0.66	13.22
		0.40	0.12	0.35			0.31	*0.19*	0.11	0.35
LMC 1	3(3)	14.20	1.16	13.89						
		0.48	0.18	0.67						
LMC 2	2(3)	14.39	1.25	13.97						
		0.33	0.16	0.54						
LMC 3	7(8)	14.27	1.19	13.93	14.3					
		0.81	0.35	0.84						
LMC 5	12(12)	14.08	1.07	13.90	14.4					
		0.39	0.17	0.54						
LMC 6	19(20)	14.11	1.03	13.98	14.8					
		0.37	0.18	0.48						
LMC 7	11(11)	14.30	1.09	14.09	14.9					
		0.50	0.17	0.70						
LMC 8	6(6)	14.08	1.01	13.98						
		0.67	0.18	0.55						
LMC 9	30(32)	13.89	1.04	13.93	14.7	30(32)	10.89	*1.49*	0.51	13.93
		0.35	0.21	0.45			0.51	*0.26*	0.16	0.45
LMC 10	32(32)	14.04	1.06	13.87	14.9					
		0.49	0.20	0.53						
LMC 11	17(19)	13.93	1.06	13.75	14.7					
		0.56	0.23	0.67						
LMC 12	19(19)	13.93	1.07	13.64	14.3	19(19)	10.56	*1.59*	0.57	13.64
		0.69	0.20	0.55			0.56	*0.37*	0.22	0.55
LMC 13	18(18)	14.17	1.01	14.07	15.6					
		0.69	0.26	0.94						
LMC 14	5(5)	13.88	0.93	13.88						
		0.34	0.12	0.40						
LMC 16	49(49)	13.79	1.02	13.66	14.6					
		0.48	0.19	0.53						
LMC 17	17(17)	13.79	1.11	13.56	14.0					
		0.53	0.15	0.38						
LMC 18	20(20)	14.00	1.12	13.75	14.5					
		0.52	0.18	0.57						
LMC 19	8(8)	13.87	1.03	13.74	14.0					
		0.28	0.16	0.38						
LMC 20	29(31)	14.02	1.06	13.84	14.8	21(31)	10.82	*1.59*	0.57	13.93
		0.49	0.17	0.50			0.55	*0.19*	0.13	0.53
	#C stars					#C stars				
LMC 21	22(23)	13.99	1.06	13.82	14.6					
		0.36	0.17	0.44						
LMC 23	20(21)	14.05	1.03	13.92	14.6					
		0.42	0.17	0.53						
LMC 24	10(10)	14.01	1.06	13.84	14.5					
		0.53	0.32	0.69						
LMC 25	5(5)	14.37	0.96	14.33						
		1.46	0.23	1.73						
LMC 27	5(5)	13.98	1.01	13.88						
		0.29	0.04	0.28						
LMC 28	36(37)	14.00	1.01	13.90	15.1					
		0.62	0.21	0.62						
LMC 29	13(13)	14.14	1.02	14.03	14.9					
		0.61	0.25	0.70						
LMC 30	32(33)	13.84	1.06	13.67	14.5					
		0.54	0.17	0.53						
LMC 31	5(5)	13.67	1.13	13.41						
		0.28	0.24	0.42						
LMC 32	24(25)	14.23	1.09	13.93	14.6	24(25)	10.86	*1.58*	0.56	13.93
		0.46	0.19	0.43			0.49	*0.34*	1.19	0.43
LMC 33	80(81)	14.04	1.10	13.83	15.0	23(81)	10.71	*1.56*	0.56	13.79
		0.47	0.21	0.46			0.45	*0.27*	0.16	0.35

TABLE 6. (continued)

	All Stars					Stars with *RI* and *JHK*				
Field	#C stars observed	I_0	$(R\text{-}I)_0$	m_{bol}	$m_{bol}(t)$	#C stars observed	K_0	$(J\text{-}K)_0$	$(H\text{-}K)_0$	m_{bol}
LMC 34	28(30)	13.95	1.09	13.74	14.4					
		0.33	0.16	0.39						
LMC 35	24(24)	13.87	1.05	13.72	14.2					
		0.36	0.18	0.39						
LMC 36	20(23)	14.08	1.11	13.84	14.5					
		0.40	0.20	0.45						
LMC 37	44(45)	14.17	1.09	13.93	15.2	24(45)	10.94	*1.49*	0.49	13.97
		0.48	0.21	0.54			0.66	*0.28*	0.17	0.53
LMC 38	22(22)	13.98	1.09	13.73	14.3	22(22)	10.71	*1.49*	0.51	13.73
		0.42	0.16	0.50			0.53	*0.33*	0.21	0.51
LMC 39	8(9)	13.99	1.03	13.86	14.3					
		0.46	0.20	0.53						
LMC 40	8(8)	13.98	1.13	13.71	14.0					
		0.32	0.17	0.35						
LMC 41	4(4)	14.09	1.08	13.90						
		0.56	0.34	0.94						
LMC 42	32(34)	14.06	1.03	13.93	15.0					
		0.43	0.22	0.57						
LMC 43	20(23)	14.00	1.04	13.86	14.9					
		0.43	0.23	0.66						
LMC 44	8(8)	13.76	1.07	13.58	14.0					
		0.34	0.26	0.53						
LMC 45	5(7)	13.56	1.07	13.38						
		0.15	0.08	0.22						
LMC 46	9(10)	13.86	1.11	13.62	14.1					
		0.41	0.19	0.54						
LMC 47	1(1)	13.79	1.21	13.42						
LMC 48	4(4)	13.86	0.97	13.81						
		0.25	0.15	0.40						
LMC 49	4(4)	14.08	1.02	13.96						
		0.10	0.22	0.37						
LMC 50	6(6)	14.36	0.90	14.40						
		0.45	0.21	0.63						
LMC 51	8(8)	13.74	1.14	13.46	13.7					
		0.23	0.19	0.33						
LMC 52	9(9)	13.90	1.01	13.79	14.2					
		0.37	0.15	0.45						
WORC	35	13.80	1.08	13.61						
		0.39	0.18	0.43						
ALL	923	13.98	1.07	13.80		197	10.73	*1.55*	0.54	13.80
STARS		0.49	0.20	0.55			0.57	*0.28*	1.74	0.50

[a]Numbers in parentheses indicate the total number of C stars identified in each field by BMB.

In order to test for systematic spatial variations in age and or metallicity amongst the fields observed, we tested the $m_{bol}(t)$ values for dependence on the position of their respective fields. Since some of the fields are centered on populous star clusters, it is possible that the number of C stars counted by BM in these fields contains a significant contribution from cluster members. If this were true it could affect the results in some unknown fashion, although BM noted that C stars which appeared to be cluster members were excluded from their counts. Thus, in addition to considering all fields from Table 6 with $m_{bol}(t)$ values, we separately analyzed only fields with no clusters. One of the main conclusions of this paper is that there is a significant (>99.5%) correlation between a field's $m_{bol}(t)$ value and its distance r from the center of the LMC. The sense of this correlation is that the transition luminosity gets brighter with increasing r. Furthermore, most of this dependence arises from the Y coordinate alone (correlation probability of 98.5%), i.e., the perpendicular distance of a field from the LMC bar. Nonparametric Spearman rank order tests and Kendall Tau tests confirm the reality of these correlations at the 98% level or greater. Figures 8(a) and 8(b) illustrate these result. For the 36 fields for which we could determine a reliable $m_{bol}(t)$, we find for the linear regression of $m_{bol}(t)$ on r and on $|Y|$:

$$m_{bol}(t) = -0.0146(\pm 0.0049) \times r + 14.935(\pm 0.149), \quad (10)$$

$$m_{bol}(t) = -0.0118(\pm 0.0046) \times |Y| + 14.721(\pm 0.096). \quad (11)$$

For the analysis for the 27 fields without clusters, a linear regression yields

$$m_{bol}(t) = -0.0144(\pm 0.0048) r + 14.865(\pm 0.136), \quad (12)$$

TABLE 7. Field positions and C and M star numbers.

Field	Field Coordinates			Numbers of Stars				C/M	Cluster	SWB	
	X	Y	r	C	M6/+	M5	(C+M)		NGC	type	
LMC 01	-3.1°	-2.9°	4.3	3	4	8	15	0.25	1651	V	4.3
LMC 02	-4.1	-1.4	4.3	3	4	6	13	0.30	1652	VI	4.3
LMC 03	-4.0	-0.1	4.0	8	4	7	19	0.73			4.0
LMC 05	-2.7	-1.1	3.0	12	8	11	31	0.63			3.0
LMC 06	-2.3	-1.4	2.7	20	8	11	39	1.05	1751	V	2.7
LMC 07	-0.4	-3.9	3.9	11	4	11	26	0.73			3.9
LMC 08	-4.1	2.1	4.6	6	5	13	24	0.33	1783	V	4.6
LMC 09	-2.6	0.0	2.6	32	12	33	77	0.71			2.6
LMC 10	-1.8	-0.9	2.0	32	14	29	75	0.74			2.0
LMC 11	-2.7	0.5	2.8	19	12	21	52	0.58	1806	V	2.8
LMC 12	-1.2	-1.5	1.9	19	12	18	49	0.63			1.9
LMC 13	-2.6	1.3	2.9	18	7	18	43	0.72	1846	V	2.9
LMC 14	-0.4	-2.2	2.2	5	5	6	16	0.45			2.2
LMC BW	-1.6	-0.1	1.6	70	38	49	157	0.80			1.6
LMC 16	-1.7	0.2	1.7	49	26	42	117	0.72			1.7
LMC 17	-2.7	0.9	2.8	16	6	11	33	0.94			2.8
LMC 18	-2.0	1.4	2.4	20	6	8	34	1.43			2.4
LMC 19	-3.0	3.3	4.5	8	2	7	17	0.89			4.5
LMC 20	-0.3	-1.1	1.1	31	12	19	62	1.00			1.1
LMC 21	-1.3	1.0	1.6	23	12	14	49	0.88			1.6
LMC R	-0.7	0.6	1.0	37	23	30	90	0.70	1917		1.0
LMC 23	0.5	-1.4	1.5	21	9	15	45	0.88			1.5
LMC 24	-1.0	1.8	2.1	10	8	5	23	0.77			2.1
LMC 25	1.3	-2.5	2.8	5	7	12	24	0.26			2.8
LMC O	0.0	0.0	0.0	79	38	63	180	0.78			0.0
LMC 27	-1.4	3.1	3.4	5	3	8	16	0.45			3.4
LMC 28	0.6	-0.8	1.0	37	17	34	88	0.73	1987	IV	1.0
LMC 29	-1.3	3.4	3.6	13	2	4	19	2.17	1978	VI	3.6
LMC 30	0.2	0.7	0.8	33	13	26	72	0.85			0.8
LMC 31	-0.5	2.9	3.0	5	3	7	15	0.50			3.0
LMC 32	0.1	1.6	1.6	25	11	17	53	0.89			1.6
LMC 33	0.9	0.1	0.9	81	33	52	166	0.95			0.9
LMC 34	1.5	-0.9	1.7	30	11	11	52	1.36			1.7
LMC 35	2.0	-1.3	2.4	24	9	15	48	1.00			2.4
LMC 36	0.9	1.6	1.9	23	10	16	49	0.88			1.9
LMC 37	1.7	0.0	1.7	45	15	36	96	0.88			1.7
LMC 38	1.3	1.2	1.7	22	6	9	37	1.47	2108	V	1.7
LMC 39	2.6	-1.7	3.1	9	6	8	23	0.64			3.1
LMC 40	0.8	2.7	2.8	8	5	7	20	0.67			2.8
LMC 41	1.0	2.7	2.9	4	5	7	16	0.33			2.9
LMC 42	2.0	0.2	2.0	34	18	24	76	0.81			2.0
LMC 43	2.5	-0.8	2.6	23	5	14	42	1.21	2121	VI	2.6
LMC 44	1.4	3.7	3.9	8	4	7	19	0.73			3.9
LMC 45	1.7	3.5	3.9	7	3	7	17	0.70	2154	V	3.9
LMC 46	1.3	5.1	5.3	10	2	6	18	1.25	2155	VI	5.3
LMC 47	3.7	-1.8	4.2	1	1	8	10	0.11	2173	V	4.2
LMC 48	3.2	0.0	3.2	4	3	5	12	0.50			3.2
LMC 49	4.8	-2.5	5.4	4	0	6	10	0.67	2209	II	5.4
LMC 50	4.3	-0.3	4.3	6	4	4	14	0.75	2213	V	4.3
LMC 51	3.6	2.2	4.2	8	3	13	24	0.50	2270	?	4.2
LMC 52	3.5	2.9	4.5	9	1	6	16	1.29			4.5

$$m_{\rm bol}(t) = -0.0121(\pm 0.0047) \times |Y| + 14.667(\pm 0.088). \quad (13)$$

These relations are displayed in Figs. 8(a) and 8(b). Clearly, there is essentially no difference between samples that include or exclude fields with populous star clusters. However, as may be seen from the figures, the fields with clusters show more scatter than do the fields without clusters. The variances in $m_{\rm bol}(t)$ for the two sets of fields are 0.32 and 0.10, respectively. We do not find any significant correlation between $m_{\rm bol}(t)$ and the X coordinate of a field or its absolute value. Nor do we find a difference between fields with and without JHK photometry.

Given the good agreement between qualitative predictions of carbon star theory and observations (FMB), particularly with regards to the occurance of a transition luminosity and its dependence on age and chemical composition, our finding that in the LMC $m_{\rm bol}(t)$ gets brighter as one moves away from the bar has at least two simple interpretations. The first is that the metallicity of the population from which the C stars are drawn increases with increasing distance from the

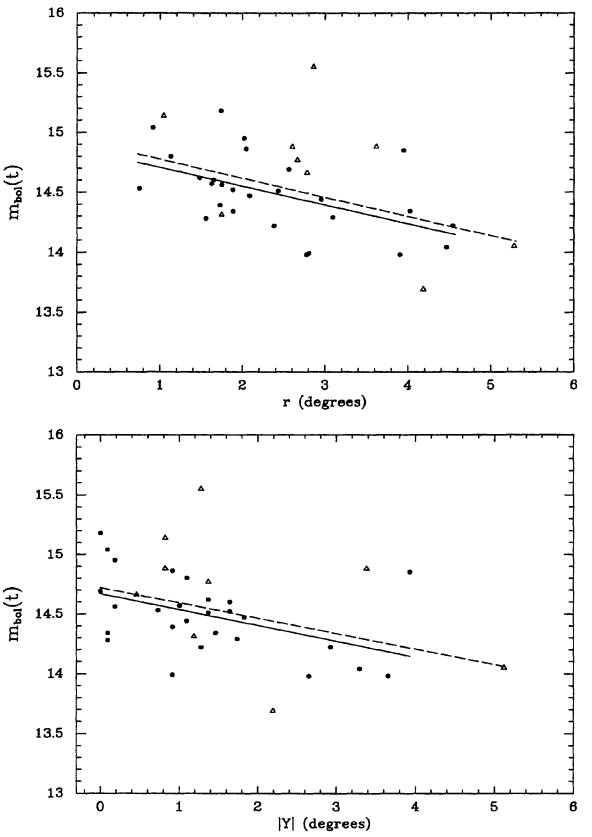

FIG. 8. (a) The transition luminosity $[m_{bol}(t)]$ for the 36 fields that satisfy the conditions imposed in Sec. 5.2, shown as a function of the field's radial distance in the plane of the sky from the center of the LMC, (r). Solid dots represent fields without clusters; open triangles fields centered on populous clusters. The dashed line is the linear regression of $m_{bol}(t)$ on r for all 36 fields [Eq. (10)]. The solid line is the same regression for the 27 fields remaining if fields with clusters are excluded [Eq. (12)]. (b) The transition luminosity $[m_{bol}(t)]$ for the same 36 fields plotted in (a), shown as a function of the field's absolute distance from the Bar of the LMC ($|Y|$). Symbol code is the same as in (a). The dashed line is the regression of $m_{bol}(t)$ on $|Y|$ for all 36 fields [Eq. (11)]; the solid line is the same regression for the 27 fields without clusters [Eq. (13)].

bar. Secondly, it is possible that the oldest epoch of star formation in each field that resulted in the formation of a significant number of C stars gets progressively younger with increasing distance from the bar. Either one of these possibilities, or a combination of the two, would result in a relative increase in stellar mass with increasing distance and thus would require that an AGB star achieve a higher luminosity before it could become a C star. This result is considered further in Sec. 6.

Since FMB demonstrated that $m_{bol}(t)$ for the clusters correlates well with SWB type, we decided to examine the dependence of the SWB cluster type itself on position. This has the advantage that the SWB type is known for clusters with few or no C stars and for clusters that have not been surveyed for C stars. We find no significant correlation between the SWB type of a cluster and either its distance perpendicular to the LMC bar or from the center of the LMC. This result may not be surprising since the total range implied by the field C stars is only one SWB type; the uncertainty in assigning an SWB type to a cluster is about one type; and there are only eight clusters of SWB type later than 5.

5.3 Correlations Involving the C and M Star Numbers

Blanco & McCarthy (1983) discussed the spatial distributions of C and M stars identified in their surveys of the LMC and SMC. They found that while the ratio of C to M5+ stars (M5 and later) declines sharply away from the SMC's center, it is nearly constant with central distance in the LMC.[6] Since we have found a dependence on central distance of the transition luminosity $m_{bol}(t)$ for LMC C stars, it seemed worthwhile to reanalyze BM's data. As in the previous section we selected only those fields with eight or more C stars so as to reduce the effects of small number statistics. Thus, this set of fields includes all of those with a value for $m_{bol}(t)$ plus two more for a total of 38 fields. For these fields, with data from Table 2 of BM (repeated here in Table 7) we find that the ratio of C to M6 and later giants (M6+) increases with r with a correlation probability of >99%; this correlation is illustrated in Fig. 9(a). The probability drops to 97.5% if only the 28 fields without clusters are considered; however, this latter correlation depends critically on the field near $r=50$ with C/M6+=9. Removal of this field also removes the correlation. Nonparametric tests (Spearman rank order and Kendall tau) do not reveal a significant correlation between C/M6+ and r whether or not fields with clusters are included in the analysis. We also note that the fields with clusters show a significantly greater scatter in the C/M6+ ratio than do fields without clusters: The mean and variance of this ratio for the 10 fields with clusters and the 28 fields without clusters are (3.29, 2.59) and (2.53, 1.96), respectively.

Figure 9(b) illustrates the radial dependence of the ratio of M6 and later giants to those of type M5. There appears to be a downward trend for this ratio at large r. Although both linear and nonparametric tests indicate significance at the 99% level for all 38 fields with 8 or more C stars in them, this drops to only the 92% or less level if fields with clusters are excluded from the analysis. The mean values of the M6+/M5 ratio and its variance for the 10 fields with clusters and the 28 fields without clusters are (0.50, 0.03) and (0.64, 0.07), respectively. Thus, we conclude that evidence for a radial dependence of the ratio of C to M stars is weak but cannot be entirely ruled out.

Finally, we find strong correlations between the ratios of C/M5 giants to that of M6+/M5 giants and between C/M6+ to M5/M6+. These are illustrated in Figs. 10(a) and 10(b). The significance of the linear correlations between these quantities is >99% if fields with clusters are excluded and only slightly less if all 38 fields with $\#C \geq 8$ are analyzed. Figure 10(a) suggests that the scatter in C/M5 may be greater

[6]The Blanco *et al.* surveys are complete for these later type M giants. Also, the later the M type the closer one gets on the AGB to the transition between M and C stars. Thus the sensitivity of the relative numbers of these stars to changes in age or metallicity of the population will increase for later stars. Thus we have concentrated on M6 and later stars so as to maximize sensitivity to changes in their parent population. In the LMC there are 2.8× as many M5 stars as M6 and later giants.

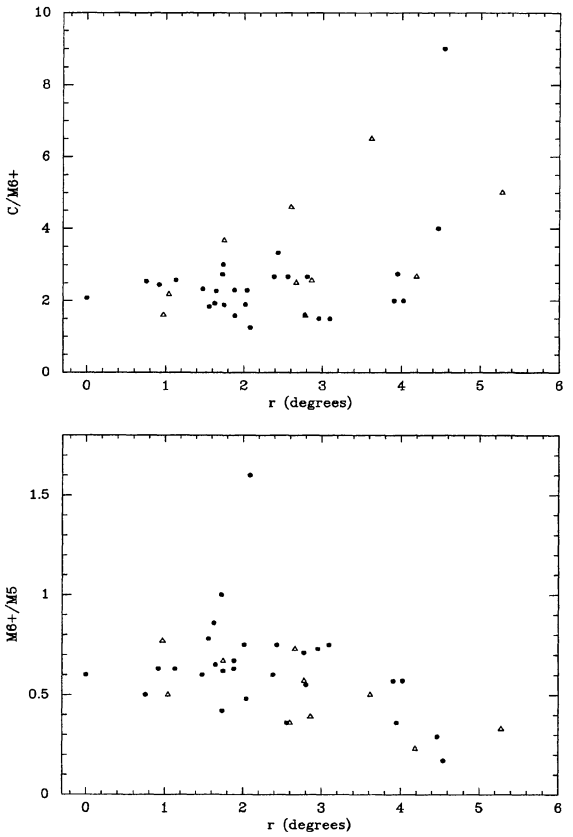

FIG. 9. (a) The ratio of C to M6 and later stars (C/M6+) for the 38 fields that satisfy the conditions imposed in Sec. *5.3*, shown as a function of the field's radial distance in the plane of the sky from the center of the LMC (r). Symbol code is the same as in Fig. 8(b) The ratio of M6 and later stars to M5 stars (M6+/M5) for the same 38 fields plotted in (a), shown as a function of r. Symbol code is the same as above.

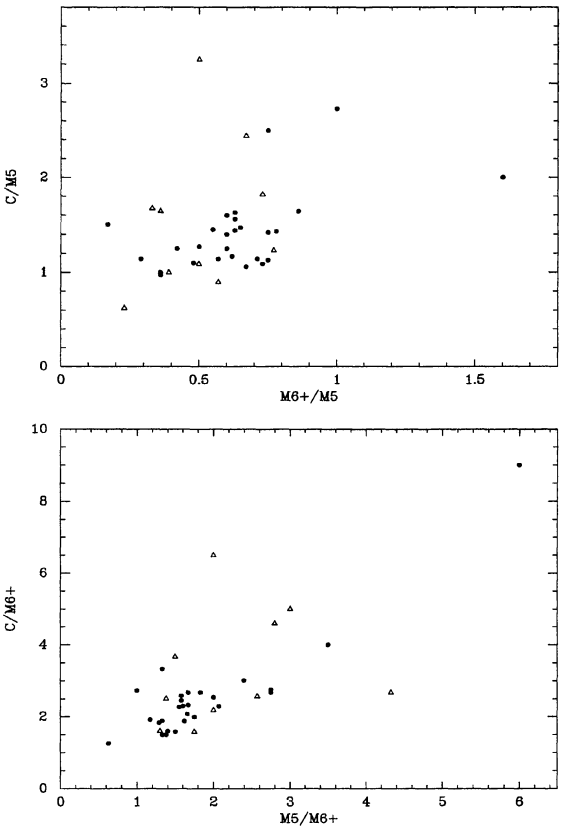

FIG. 10. (a) The ratio of C to M5 stars (C/M5) for the 38 fields that satisfy the conditions imposed in Sec. *5.3*, shown as a function of the ratio between M6 and later stars and M5 stars, (M6+/M5). Symbol code is the same as in Fig. 8(b) The ratio of C to M6 and later stars (C/M6+) for the same 38 fields plotted in (a), shown as a function of the ratio between M5 and M6 and later stars, (M5/M6+). Symbol code is the same as above.

for the cluster fields than the noncluster fields. The mean and variance in this ratio for the two groups of fields are (1.57, 0.62) and (1.42, 0.17), respectively. For all 38 fields the linear least-squares solutions are

$$(\mathrm{C/M6+})=0.58(\pm0.38)+1.09(\pm0.17)\times(\mathrm{M5/M6+}), \quad (14)$$

$$(\mathrm{C/M5})=0.98(\pm0.22)+0.80(\pm0.34)\times(\mathrm{M6+/M5}). \quad (15)$$

For the 28 fields without clusters, the solutions are

$$(C/\mathrm{M6+})=0.15(\pm0.24)+1.28(\pm0.12)\times(\mathrm{M5/M6+}), \quad (16)$$

$$(C/\mathrm{M5})=0.87(\pm0.18)+0.86(\pm0.27)\times(\mathrm{M6+/M5}). \quad (17)$$

Either pair of solutions suggests that as the ratio of M6+/M5 stars increases due, for example, to changes in age or chemical composition, the C/M5 ratio will increase somewhat more slowly.

6. SUMMARY AND CONCLUSIONS

6.1 The Luminosities and Colors of the C Stars

The bolometric luminosity function for our unbiased sample of 895 C stars (Fig. 4 and Table 4) is nearly the same as that for populous LMC clusters (FMB) and that of CFPE. Our new results particularly emphasize the nearly complete absence of C stars with $m_{\mathrm{bol}} \leqslant 12.5$. Combined with results from Frogel & Blanco (1990) on field M stars and from FMB for clusters, we conclude that one or more processes such as a superwind phase or convective overshooting must combine to strongly inhibit any AGB star in the LMC from becoming more luminous than $M_{\mathrm{bol}} \approx -6$. Our results are consistent with the survey of Reid *et al.* (1990) for luminous AGB stars in the LMC and Reid & Mould's (1990) in the SMC (see also Wood *et al.* 1992 on upper limits to the luminosity of OH/IR stars).

There are a substantial number of C stars in our field sample with $J-K \geqslant 1.9$; such stars are almost completely absent from SWB IV–VI clusters. This fact and a similar excess of red and luminous field M giants compared with SWB IV–VI clusters (Frogel & Blanco 1990) could arise if

the metallicity distribution for field stars was skewered to higher values than that for cluster stars (Sec. 3.1). Higher metallicity produces more luminous M stars by raising the transition luminosity between M and C stars. This explanation raises the interesting question of why should the field have a metallicity distribution skewed to higher values than that of the clusters. A comparison of the luminous CH stars found by Hartwick & Cowley (1988) and studied in the IR by SPE and Feast & Whitelock (1992) with the C stars studied here leads us to conclude that these CH stars are the blue tail of the distribution of C stars found in the BMB and BM surveys and do not represent a distinct class of stars.

Finally, from a comparison of the $M_{\rm bol}$, $T_{\rm eff}$ diagram for C stars with models, we conclude that a 1 $M_\odot$ model does indeed represent the lower mass limit for a moderately metal-poor C star (cf. Lattanzio 1989a; FMB). For lower masses, dredge-up of processed material is not sufficient to make C/O>1 in the envelope. To turn a more metal-rich or younger (i.e., more massive) M star into a C star requires a combination of higher luminosity and lower temperature.

6.2 The M to C Star Transition Luminosity and its Spatial Distribution

The transition luminosities between field M stars and C stars correspond to those in Magellanic Cloud clusters of SWB types V–VI, significantly fainter than those of types III–IV. Given the close linkage between age and metallicity for the clusters (e.g., Cohen 1982; Bica *et al.* 1986) this result implies that throughout the LMC there is a significant population of stars similar to those found in the older, metal-poor end of the distribution of intermediate age LMC clusters. In other words, none of the fields surveyed by BM has an exclusively younger stellar population such as is found in clusters of SWB type II–IV.

There is a significant brightening of $m_{\rm bol}(t)$ with increasing distance from the center of the LMC. The change in $m_{\rm bol}(t)$ is from ~14.7 near the bar to ~14.1 in the outermost fields [Figs. 8(a), (b)]. If we compare this with the relation between $m_{\rm bol}(t)$ and turnoff mass in Fig. 19 of FMB, we can estimate the oldest epoch of C star formation as a function of position. We conclude that for the same [Fe/H] versus age relation as the clusters, the earliest epoch of C star formation in the field near the bar of LMC corresponds to clusters of SWB type 6.5 while near the periphery it corresponds to clusters of SWB 5.5, or an age difference of a few Gyr according to Table 3 of FMB (a younger "earliest epoch" on the periphery than near the bar) and an [Fe/H] difference of 0.2–0.4 dex (a higher [Fe/H] near the periphery. If the mean [Fe/H] at the periphery were forced to be the same as that near the bar, the implied age difference would be greater, i.e., the periphery would be younger still.

C stars are just the tip of the iceberg that represents the major epoch of star formation that occured a few Gyr ago in the LMC and first identified by Butcher (1977). Our finding of a systematic spatial variation in the transition luminosity between M and C stars suggests that this epoch occured somewhat more recently in the periphery of the LMC than in its central regions. This result could be tested by obtaining optical CMDs that include the main sequence turnoff for a sufficient number of LMC fields. Given the variation in $m_{\rm bol}(t)$, one would expect to find a variation in the C to M star ratio as well. However, based on the small size of the change in $m_{\rm bol}(t)$, examination of the cluster data in FMB indicates that the absence of a variation in the C to M star ratio (BM and Sec. 5 here) is not unexpected and can be attributed to statistical fluctuations in star numbers. BM did find large spatial gradients in the C to M star ratio in the SMC. Thus it could be useful to carry out a study similar to ours of the C stars found by BM and BMB in the SMC.

We are indebted to Victor Blanco for his interest in this program and for the loan of his findings charts for the LMC C stars. It was at his urging that both of us separately undertook this program and eventually came to collaborate on it. We are also grateful for the able assistance of many CTIO telescope operators without whom a program consisting of observing so many different objects would could have gone much less rapidly than it did. J.A.F.'s research on cool stars at OSU is supported by NSF Grant No. AST92-18281. He also thanks Roger Davies and PPARC for partial support via a Visiting Senior Research Fellowship at the University of Durham where this paper was prepared.

REFERENCES

Bessell, M. S. 1991, A&A, 242, L17
Bessell, M. S., Wood, P. R., & Lloyd Evans, T. 1983, MNRAS, 202, 59
Bica, E., Dottori, H., & Pastoriza, M. 1986, A&A, 156, 261
Blanco, V. M., McCarthy, M. F., & Blanco, B. M. 1980, ApJ, 242, 938 (BMB)
Blanco, V. M., & McCarthy, M. F. 1983, AJ, 88, 1442 (BM)
Blanco, V. M., & McCarthy, M. F. 1990, AJ, 100, 674
Brunet, J. P. 1975, A&A, 43, 345
Butcher, H. 1977, ApJ, 216, 372
Cohen, J. G. 1982, ApJ, 258, 143
Cohen, J. G., Frogel, J. A., Persson, S. E., & Elias, J. H. 1981, ApJ, 249, 481 (CFPE)
Costa, E. 1990, PASP, 102, 789
Cousins, A. W. J. 1974, MNASSA, 33, 149
Cousins, A. W. J. 1976a, MmRAS, 81, 25
Cousins, A. W. J. 1978, MNASSA, 37, 8
Cousins, A. W. J. 1980a, South African Astron. Obs. Circ., 1, 234
Cousins, A. W. J. 1980b, MNASSA, 39, 22
Elias, J. H., Frogel, J. A., Mathews, K., & Neugebauer, G. 1982, AJ, 87, 1029
Elias, J. H., Frogel, J. A., Hyland, A. R., & Jones, T. J. 1983, AJ, 88, 1027
Feast, M., & Whitelock, P. 1992, MNRAS, 259, 6
Frogel, J. A., & Blanco, V. M. 1990, ApJ, 365, 168
Frogel, J. A. Mould, J., & Blanco, V. M. 1990, ApJ, 352, 96 (FMB)
Frogel, J. A., Persson, S. E., Aaronson, M., & Matthews, K. 1978, ApJ, 220, 75
Frogel, J. A., Persson, S. E., & Cohen, J. G. 1980, ApJ, 239, 495
Frogel, J. A., & Richer, H. B. 1983, ApJ, 275, 84
Graham, J. A. 1982, PASP, 94, 244
Groenewegen, M. A. T., & de Jong, T. 1993, A&A, 67, 410
Groenewegen, M. A. T., van den Hoek, L. B., & de Jong, T. 1995, A&A, 293, 381

Hartwick, F. D. A., & Cowley, A. P. 1988, ApJ, 334, 135
Hardie, R. H. 1962, in Stars and Stellar Systems, Vol. 2, Astronomical Techniques, edited by W. A. Hiltner (University of Chicago, Chicago), p. 178
Iben, Jr., I., 1981, ApJ, 246, 278
Iben, Jr., I., & Renzini, A. 1983, ARA&A, 21, 271
Iben, Jr., I., Progress and Opportunities in Southern Hemisphere Optical Astronomy, in ASP Conf. Ser. 1 (ASP, San Francisco), p. 220
Johnson, H. L. 1964, Bull. Tonantzintla and Tacubaya Obs., 3, 305
Jones, T. H., & Hyland, A. R. 1980, MNRAS, 192, 359
Lattanzio, J. C. 1986, ApJ, 311, 708
Lattanzio, J. C. 1989a, ApJ, 344, L25
Lattanzio, J. C. 1989b, in Evolution of Peculiar Red Giant Stars, edited by H. R. Johnson & B. Zuckerman (Cambridge University Press, Cambridge), p. 161
Lattanzio, J. C. 1991, ApJS, 76, 215
Mendoza, E. E., & Johnson, H. L. 1965, ApJ, 141, 161
Rebeirot, E., Azzopardi, M., & Westerlund, B. E. 1993, A&AS, 97, 603
Reid, N., & Mould, J. 1990, ApJ, 360, 490
Reid, N., Tinney, C., & Mould, J. 1990, ApJ, 348, 98
Renzini, A., & Voli, M. 1981, A&A, 94, 175
Richer, H. B. 1981, ApJ, 243, 744
Ridgway, S. T., Jacoby, G. H., Joyce, R. R., & Wells, D. C. 1980a, AJ, 85, 1496
Ridgway, S. T., Joyce, R. R., White, N. M., & Wing, R. F. 1980b, ApJ, 235, 126
Sanduleak, N., & Philip, A. G. D. 1977, Pub. Warner and Swasey Obs., 2, 105 Scalo, J. M. 1976, ApJ, 206, 474
Scalo, J. M. 1976, ApJ, 206, 474
Searle, L., Wilkinson, A., & Bagnuolo, W. G. 1980, ApJ, 239, 803 (SWB)
Suntzeff, N. B., Phillips, M. M., Elias, J. H., Cowley, A. P., Hartwick, F. D. A., & Bouchet, P. 1993, PASP, 105, 350
Wallerstein, G. 1973, ARA&A, 11, 115
Westerlund, B. E., Azzopardi, M., & Breysacher, J. 1986, A&AS, 65, 79
Westerlund, B. E., Olander, N., Richer, H. B., & Crabtree D. R. 1978, A&AS, 31, 61
Westerlund, B., E., Azzopardi, M., Breysacher, J., & Rebeirot, E. 1991 A&AS 91, 425
Westerlund, B., E., Azzopardi, M., Breysacher, J., & Rebeirot, E. 1995 A&AS, 303, 107
Wood, P. R., Whiteoak, J. B., Hughes, S. M. G., Bessell, M. S., Gardner, F. F., & Hyland, A. R. 1992, ApJ, 397, 552